

# ALTERATIONS IN RESPIRATORY MECHANICS AND GAS EXCHANGE IN MODELS OF TREATED AND UNTREATED TYPE 2 DIABETES

Álmos István Schranc MD

PhD Thesis

Department of Medical Physics and Informatics  
Department of Anaesthesiology and Intensive Therapy

University of Szeged, Hungary  
Albert Szent-Györgyi Medical School  
Doctoral School of Theoretical Medicine



Supervisors:

Prof Ferenc Peták PhD DSc

Prof Barna Babik MD PhD

Szeged, 2022

**LIST OF SCIENTIFIC PUBLICATIONS INCLUDED IN THE PRESENT THESIS****I. Lung and chest wall mechanical properties in metformin-treated and untreated models of type 2 diabetes**

Álmos Schranc, Gergely H. Fodor, Roberta Südy, Bence Ballók, Richard Kulcsár, József Tolnai, Barna Babik, Ferenc Peták

Journal of Applied Physiology, 2022; 132(5):1115-1124

**II. Exaggerated ventilator-induced lung injury in an animal model of type 2 diabetes mellitus: a randomized experimental study**

Álmos Schranc, Gergely H. Fodor, Roberta Südy, József Tolnai, Barna Babik, Ferenc Peták

Frontiers in Physiology, 2022; 13:889032

**LIST OF SCIENTIFIC PUBLICATIONS RELATED TO THE SUBJECT OF THE PRESENT THESIS:****III. Lung volume dependence of respiratory function in rodent models of diabetes mellitus**

Roberta Südy, Álmos Schranc, Gergely H. Fodor, József Tolnai, Barna Babik, Ferenc Peták

Respiratory Research, 2020; 21(1):82

## TABLE OF CONTENTS

<b>LIST OF SCIENTIFIC PUBLICATIONS INCLUDED IN THE PRESENT THESIS .....</b>	<b>1</b>
<b>LIST OF SCIENTIFIC PUBLICATIONS RELATED TO THE SUBJECT OF THE PRESENT THESIS: .....</b>	<b>1</b>
<b>TABLE OF CONTENTS .....</b>	<b>2</b>
<b>LIST OF FIGURES AND TABLES .....</b>	<b>4</b>
<b>GLOSSARY OF TERMS .....</b>	<b>5</b>
<b>I. INTRODUCTION .....</b>	<b>6</b>
I.1. Epidemiology of type 2 diabetes .....	6
I.2. Pathophysiology of type 2 diabetes .....	6
I.2.1. Genetic susceptibility and related beta cell dysfunction .....	7
I.2.2. Environmental factors in T2DM development .....	8
I.3. Respiratory system alterations in presence of type 2 diabetes .....	9
I.3.1. Skeletal muscle function in T2DM .....	9
I.4. Metformin therapy .....	10
I.5. Ventilator-induced lung injury .....	10
<b>II. AIMS AND HYPOTHESES .....</b>	<b>13</b>
II.1. Effect of T2DM on the PEEP-dependent respiratory mechanics .....	13
II.2. Modulation of VILI in models of treated and untreated T2DM .....	14
<b>III. MATERIALS AND METHODS .....</b>	<b>15</b>
III.1. Ethical considerations .....	15
III.2. Pretreatments .....	15
III.3. Group allocations and exclusions .....	16
III.4. Animal preparations .....	17
III.5. Blood gas measurements and intrapulmonary shunt fraction calculation .....	17
III. 6. Measurement of respiratory mechanics .....	18
III.6.1. Separation of chest wall and lung mechanics .....	19
III.6.2. Model fitting to the total respiratory impedance spectra .....	19
III. 7. Lung section preparation and histological analysis .....	20
III.7.1. Effect of T2DM on the PEEP-dependent respiratory mechanics .....	20
III.7.2. Modulation of VILI in models of treated and untreated T2DM .....	20
III. 8. Additional measurements .....	21
III.8.1. Thoracic gas volume .....	21
III.9. Experimental protocols .....	22
III.9.1. Effect of T2DM on the PEEP-dependent respiratory mechanics .....	22
III.9.2. Modulation of VILI in models of treated and untreated T2DM .....	23
III.10. Statistical analysis .....	23
III.10.1. Effect of T2DM on the PEEP-dependent respiratory mechanics .....	24
III.10.2. Modulation of VILI in models of treated and untreated T2DM .....	24
<b>IV. RESULTS .....</b>	<b>25</b>
IV.1. Effect of T2DM on the PEEP-dependent respiratory mechanics .....	25
IV.1.1. Body weights and results of IPGTTs .....	25
IV.1.2. Thoracic gas volumes .....	26
IV.1.3. Mechanical impedance data and model fitting performance .....	26

IV.1.4. Lung and chest wall mechanical parameters.....	27
IV.1.5. Gas exchange parameters .....	28
IV.1.6. Haemodynamics .....	29
IV.1.7. Lung histological findings.....	30
IV.2. Modulation of VILI in models of treated and untreated T2DM.....	31
IV.2.1. Results of IPGTTs.....	31
IV.2.2. Gas exchange parameters .....	32
IV.2.3. Respiratory mechanical alterations .....	33
IV.2.4. Lung injury score – results of histological analysis .....	33
IV.2.5. Number of 8-OHDG positive cells – results of immunohistochemistry .....	35
<b>V. DISCUSSION .....</b>	<b>36</b>
V.1. Effect of T2DM on the PEEP-dependent respiratory mechanics .....	36
V.1.1. Respiratory mechanical consequences .....	37
V.1.2. Effects of metformin therapy.....	38
V.2. Modulation of VILI in models of treated and untreated T2DM.....	39
V.2.1. VILI in the presence of T2DM .....	39
V.2.2. Effects of metformin therapy.....	40
V.3. Limitations of the studies.....	41
V.3.1. Effect of T2DM on the PEEP-dependent respiratory mechanics .....	41
V.3.2. Modulation of VILI in models of treated and untreated T2DM.....	42
<b>VI. SUMMARY AND CONCLUSIONS.....</b>	<b>42</b>
<b>VII. ACKNOWLEDGEMENTS .....</b>	<b>45</b>
<b>VIII. REFERENCES.....</b>	<b>46</b>

## LIST OF FIGURES AND TABLES

Figure 1. Schematic of insulin production and secretion .....	7
Figure 2. Alveolar changes related to VILI.....	11
Figure 3 Scheme of the pretreatment period .....	16
Figure 4. Scheme of the forced oscillatory measurement apparatus .....	18
Figure 5. Scheme of the measurement setup for the assessment of thoracic gas volume .....	22
Figure 6. Protocol scheme: Effect of T2DM on the PEEP-dependent respiratory mechanics .....	22
Figure 7. Protocol scheme: Modulation of VILI in models of treated and untreated T2DM... ..	23
Table 1. AUCs of the first and second IPGTT .....	25
Table 2. The thoracic gas volume normalized to the body mass.....	26
Figure 8. Mechanical impedance spectra in a representative rat.....	26
Table 3. Fitting errors .....	27
Figure 9. Lung and chest wall mechanical parameters at different PEEP levels .....	28
Figure 10. Gas-exchange parameters obtained at different PEEP levels .....	29
Figure 11. Mean linear intercept and differences in collagen expression in lung tissue.....	30
Figure 12. Serum glucose levels and the corresponding AUC values during IPGTTs .....	31
Figure 13. Gas exchange parameters during normal- and after injurious ventilation .....	32
Figure 14. Respiratory mechanics obtained during normal- and injurious ventilation .....	33
Figure 15. Ling injury scores and representative images .....	34
Figure 16. Number of 8-OHDG positive cells and representative images .....	35

## GLOSSARY OF TERMS

8-OHDG: 8-hydroxy-2'-deoxyguanosine	IPGTT: intraperitoneal glucose tolerance test
AGE: advanced glycation end product	IR: insulin resistance
ALI: acute lung injury	<i>iv</i> : intravenous
AMP: adenosine monophosphate	K <sup>+</sup> : ionized potassium
ANOVA: analysis of variance	LIS: lunge injury score
ARDS: acute respiratory distress syndrome	MET: metformin group
ARRIVE: animal research: reporting of in vivo experiments	mRNA: messenger ribonucleic acid
ATP: adenosine triphosphate	nTGV: normalized thoracic gas volume
AUC: area under the curve	NV: ventilation with physiological parameters
BG: blood gas	OGTT: oral glucose tolerance test
Ca <sup>2+</sup> : ionized calcium	PaO <sub>2</sub> : arterial partial pressure of oxygen
CaO <sub>2</sub> : arterial oxygen content	P <sub>A</sub> O <sub>2</sub> : alveolar partial pressure of oxygen
CcO <sub>2</sub> : capillary oxygen content	P <sub>box</sub> : plethysmography box pressure
CTRL: control group	PEEP: positive end-expiratory pressure
CvO <sub>2</sub> : venous oxygen content	P <sub>es</sub> : oesophageal pressure
DAB: diaminobenzidine	PFA: paraformaldehyde
DNA: deoxyribonucleic acid	Ptr: tracheal pressure
ECM: extracellular matrix	Q <sub>s</sub> /Q <sub>t</sub> : intrapulmonary shunt
ER: endoplasmic reticulum	RBC: red blood cell
η: tissue hysteresivity	RN: resistance
FOT: forced oscillation technique	SaO <sub>2</sub> : arterial oxygen saturation
G: tissue damping	STZ: streptozotocin
G <sub>rs</sub> : tissue damping of the total respiratory system	T2DM: type 2 diabetes; untreated type 2 diabetes group
GWASs: genome-wide association studies	TCA: tricarboxylic acid
H: tissue elastance	TGV: thoracic gas volume
HbA1c: haemoglobin A1c	VILI: ventilator-induced lung injury
H <sub>rs</sub> : tissue elastance of the total respiratory system	VT: tidal volume
IFG: impaired fasting glucose	Z <sub>cw</sub> : mechanical impedance of the chest wall
IGT: impaired glucose tolerance	ZL: lung input impedance
IIS: impaired insulin secretion	Z <sub>rs</sub> : input impedance of the respiratory system

## **I. INTRODUCTION**

### ***1.1. Epidemiology of type 2 diabetes***

Type 2 diabetes mellitus (T2DM) is a complex metabolic disorder, characterized by hyperglycaemia, insulin resistance and relative impairment in insulin secretion<sup>1</sup>. T2DM accounting for over 90% of all diabetes worldwide, therefore it is the most common type. The prevalence of T2DM is high. According to the IDF Diabetes Atlas, published in 2021, 537 million adults live with diabetes, and this number is rising globally due to various socio-economic and environmental factors, such as population aging, economic development and increasing urbanisation. By 2030, the predicted number of diabetic patients will reach 643 million and rises further to 783 million by 2045<sup>2</sup>. Furthermore, in children and adolescents, T2DM has also become a concern as a result of an increasing prevalence of obesity due to more sedentary lifestyles and greater consumption of unhealthy foods<sup>3,4</sup>.

Prediabetes is a commonly used term for impaired glucose tolerance (IGT) and impaired fasting glucose (IFG). The common feature of this conditions is the raised blood glucose level above the normal range, but not reaching the diagnostic threshold of diabetes<sup>5</sup>. Prediabetes has three major epidemiological characteristics. First, IGT and IFG signify a higher risk for the future development of T2DM<sup>6,7</sup>. Second, IGT and IFG indicate a heightened risk for cardiovascular morbidities<sup>8</sup>. Finally, the early detection of prediabetes can lead to the prevention of T2DM development<sup>9,10</sup>.

### ***1.2. Pathophysiology of type 2 diabetes***

The pathogenesis of T2DM is heterogeneous. The two main pathophysiological alterations in T2DM are impaired insulin secretion (IIS) and insulin resistance (IR)<sup>11</sup>. The combination of these adverse phenomena generates a vicious cycle of hyperglycaemia, where there is a augmented demand to decrease blood glucose level with insulin mediated by IR, and due to the IIS related to the loss of the ability of beta cells to produce the required quantity of insulin<sup>12</sup>. The early stages of T2DM development are highly influenced by genetic factors on insulin secretion<sup>13</sup>. The chronic hyperglycaemia in the subsequent phases of the pathogenesis of T2DM may induce further pancreatic beta cell dysfunctions<sup>14</sup>. Aging and genetic factors have a lower influence on IR, thus, environmental factors have the major contribution to the development of IR, such as overeating, sedentary lifestyle and resulting obesity<sup>15</sup>.

### 1.2.1. Genetic susceptibility and related beta cell dysfunction

Although the environmental factors are predominant in the development of T2DM, a complex polygenic background has been also proven. Since 2014 genome-wide association studies (GWASs) revealed almost 100 genomic loci convincingly associated with T2DM and metabolic syndrome<sup>16</sup>. A majority of the genetic variants discovered in the first GWASs affected directly the beta cell function due to a decrease in glucose-stimulated insulin response<sup>17</sup>. However, more recent studies demonstrated further genomic loci associated not only with T2DM, but also with glucose homeostasis affecting fasting glucose level, fasting insulin level, dynamics of glucose level during oral glucose tolerance test (OGTT) and the level of haemoglobin A1c (HbA1c)<sup>18,19</sup>. Furthermore, a group of these genetic variants has specific thresholds at which the genetic effect sets in and may not exert general modifying effects on fasting glucose levels in the population. Therefore, patients may live with normal fasting glucose level, however their insulin response is insufficient<sup>20</sup>.

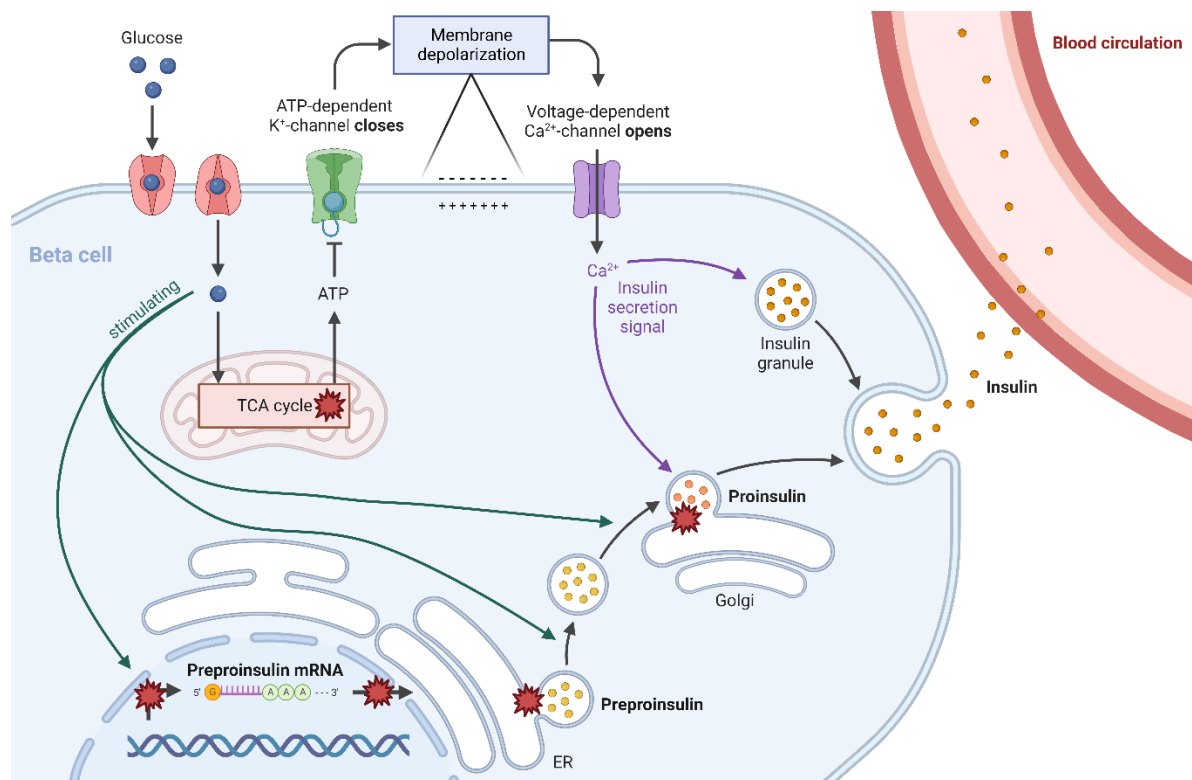


**Figure 1. Schematic of insulin production and secretion**

Main steps of insulin production and secretion by the pancreatic beta cells. Steps affected by genetic changes leading to beta cell dysfunction are marked with a red star-like symbol. Abbreviations: TCA cycle, tricarboxylic acid cycle; ATP, adenosine triphosphate;  $K^+$ , ionized potassium;  $Ca^{2+}$ , ionized calcium; mRNA, messenger ribonucleic acid; ER, endoplasmic reticulum. This figure was made in BioRender.

Insulin production and release mechanisms are demonstrated on Figure 1. Briefly, the blood glucose level increases, then the beta cells take up glucose through glucose transporter 2. Using intracellular and mitochondrial pathways, glucose is degraded. The produced ATP depolarizes the cell membrane, due to the inhibition of ATP-dependent  $K^+$ -channels. Subsequently, a voltage-dependent  $Ca^{2+}$ -channel opens, which induce the docking mechanism of the insulin containing granules<sup>21,22</sup>. Genetic variations may affect several steps of production such as transcription, mRNA translation, proinsulin folding in the endoplasmic reticulum (ER) or proinsulin conversion into insulin<sup>23</sup>.

Previous studies have been demonstrated that a reduction in beta cell mass and pancreatic insulin content was observed in patients with T2DM, due to increased beta cell apoptosis and amyloid deposition<sup>24,25</sup>. However, based on recent studies, reduction in beta cell mass is more typical in longer duration of T2DM and the dysfunction of beta cells take predominant responsibility in the development of the disease<sup>26,27</sup>. According to some estimates, 80% reduction in beta cell function could be observed at T2DM onset<sup>28</sup>. In type 1 diabetes, the causative factors of beta cell dysfunction and death can be common, whereas inducing factors in T2DM such as high levels of free fatty acids may elicit ER stress and related impairment in beta cell function without inducing cell death, thus, beta cell apoptosis in T2DM is an infrequent event<sup>29</sup>.

### *1.2.2. Environmental factors in T2DM development*

Previous studies demonstrated that the development of T2DM is related to increased weight gain and decreased physical activity<sup>30</sup>. The main risk factor for T2DM is obesity, which associated with metabolic abnormalities due to IR. Numerous factors play a determining role in the development of IR, involving both cell-autonomous and inter-organ mechanisms. Nevertheless, the exact mechanism which describes how obesity induces T2DM and IR remains unknown.

Sedentary lifestyle also plays a major role in T2DM development<sup>31</sup>. Three protective mechanisms fail in the absence of physical activity. First, in the lack of skeletal muscle contraction, the tissue blood flow decreases, thus, the glucose uptake from plasma will be reduced, resulting in higher blood glucose level<sup>32</sup>. Second, intra-abdominal fat accumulation, often termed visceral obesity, which is a high-risk factor of IR, is more common in the absence of physical activity<sup>33</sup>. Due to enhanced macrophage infiltration and activation the release of inflammatory cytokines increase along with the decrease of protective adipokine, adiponectin

production<sup>34</sup>. According to the overflow hypothesis, the adipose organ loses the ability to store further fatty acids. The capacity of the fat cells to store triglycerides exceeds and the fat overflows to the muscles and liver. Subsequently, the intracellular triglyceride metabolism interferes with insulin signalling, glucose transport and phosphorylation. Furthermore, the glycogen synthesis is increased in muscles and hepatic gluconeogenesis is augmented<sup>35</sup>. Finally, the anti-inflammatory effect of moderate intensity exercises may not be able to reduce oxidative stress, which is also a predisposing factor of T2DM<sup>36</sup>.

### ***1.3. Respiratory system alterations in presence of type 2 diabetes***

Long-term hyperglycaemia in T2DM leads to chronic inflammation by activating various cellular and molecular pathways, including the promotion of advanced glycation end products (AGEs) formation and oxidative stress<sup>37,38</sup>, disturbances of the nitric oxide – endothelin-1 balance<sup>39</sup>, an abnormal plasma lipid profile, cytokine recruitment, and activation of nuclear factor- $\kappa$ B<sup>40</sup>, in addition to proinflammatory gene expression<sup>41</sup>. Consequently, several organs are affected by T2DM because of endothelial and smooth muscle cell dysfunction and extracellular matrix (ECM) remodeling<sup>42</sup>. The whole circulatory minute volume is received by the lungs as a single organ, so their microvascular area is large, and they contain high numbers of endothelial and smooth muscle cells. Therefore, metabolic diseases have respiratory consequences<sup>43-46</sup>. Accordingly, the lung manifestations of diabetes have been presented in previous *ex vivo*<sup>47</sup> and *in vivo* studies<sup>48,49</sup>. The reported mechanical changes in respiratory mechanics, such as elevations of bronchial smooth muscle tone and adverse alterations of lung tissue viscoelasticity have clinical relevance in patient care and in guiding therapy in patients with T2DM<sup>50</sup>.

#### ***1.3.1. Skeletal muscle function in T2DM***

Skeletal muscle plays an important role in glucose homeostasis, and insulin resistance of the skeletal muscle cells is the foremost cause of T2DM development<sup>51-53</sup>. Therefore, diabetes also leads to functional and structural changes in skeletal muscle<sup>54</sup>, due to elevated plasma levels of dicarbonyl metabolites<sup>55</sup> leading to ECM remodelling and muscle loss by prolonged activation of receptor for AGEs<sup>56</sup>. Because the chest wall is a major compartment of the respiratory system, the aforementioned pathologies may also affect the diaphragm and the pectoral and intercostal respiratory muscles. Indeed, the involvement of chest wall properties in T2DM-related respiratory abnormalities can also be anticipated from AGEs accumulation in the skeletal muscles<sup>57</sup>, in association with the increased passive stiffness and overexpression of the

skeletal muscle fibres of ECM<sup>53</sup>. As the total work of breathing includes the work needed to overcome the resistive losses and elastic recoil of the lungs and chest wall<sup>58-60</sup>, characterizing the individual involvement of these compartments in respiratory dysfunction related to diabetes is of major importance. However, the primary cause of compromised respiratory function in long term hyperglycaemia has not been elucidated, and there is a particular lack of knowledge regarding the contribution of the lung and chest wall compartments to the overall changes in the respiratory system.

#### ***1.4. Metformin therapy***

Metformin is the first-line therapeutic agent for suppressing the T2DM-related pathologies mentioned above. Metformin has one primary and two secondary methods for decreasing blood glucose level<sup>61</sup>. The main mechanism is due to directly affecting hepatic glucose production, as opposed to augmenting insulin secretion or increasing glucose disposal<sup>62</sup>. The possible pharmacodynamics are the following. Metformin inhibits Complex I in the mitochondrion, thereby alters hepatic adenine nucleotide energy charge due to decreased electron transport chain activity, which can potentially mediate the antidiabetic effects of metformin<sup>63</sup>. Furthermore, the abovementioned effect results in adenosine monophosphate kinase activation, which reduces hepatic glucose production due to downregulation of gluconeogenic genes<sup>64</sup> and reduces hepatic diacylglycerol content along with improving hepatic insulin sensitivity, due to reduced lipogenesis and improved hepatic mitochondrial oxidation<sup>65</sup>. The third, and most recent theory is that metformin inhibits glycerol-3-phosphate dehydrogenase and thereby upsets the cytosolic and mitochondrial redox balance<sup>61</sup>. As secondary effects, metformin increase insulin-stimulated glucose uptake<sup>66</sup> and alters intestinal glucose absorption due to changes in gut microbiome composition<sup>67</sup> and hormone secretion<sup>68</sup>.

Previous studies reported the preventing effects of metformin against the development of systemic T2DM complications<sup>69</sup>. Furthermore, the control of hyperglycaemia in the presence of T2DM, in patients receiving metformin improves survival following respiratory infections and inhibits the progression of lung fibrosis<sup>70</sup>. However, the mechanism of metformin treatment on the respiratory consequences of diabetes have not been explored.

#### ***1.5. Ventilator-induced lung injury***

Ventilator-induced lung injury (VILI) commonly may occur due four major mechanisms. Three of them induced by physical forces such as barotrauma, volutrauma and atelectrauma and lastly the predominantly consequent biotrauma<sup>71</sup>. As less frequent etiologies, adverse heart-lung

interactions, deflation related, and effort induced injuries can be also responsible for VILI development.

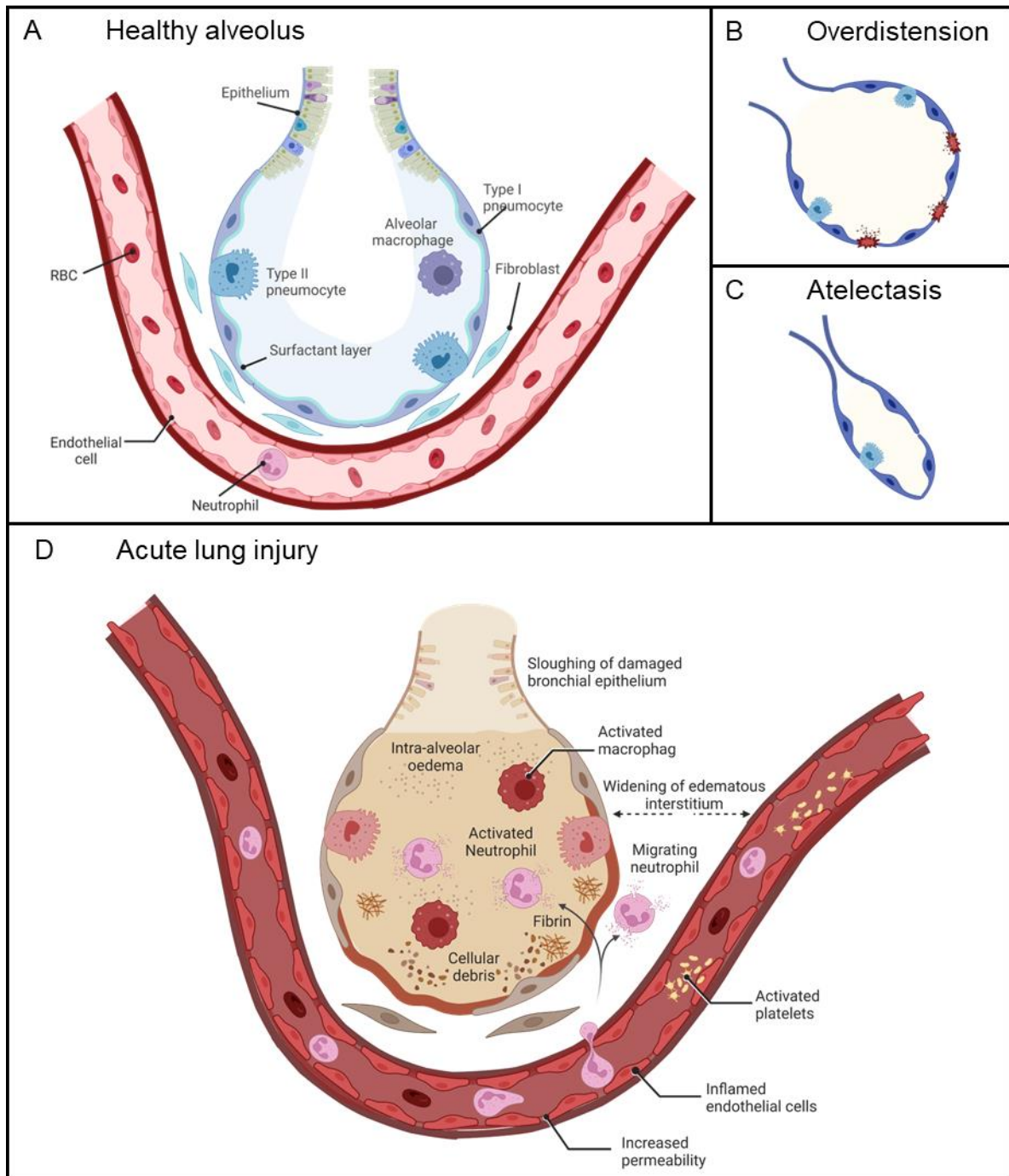


**Figure 2. Alveolar changes related to VILI**

*A: Healthy alveolus and adjacent capillary. B: Overdistension due to high tidal volumes or high transpulmonary pressures and related alveolar wall damage. C: Atelectasis due to insufficient tidal volume or PEEP. D: Main alveolar changes in acute lung injury. Abbreviation: RBC, red blood cell. This figure was made in BioRender.*

Pressure related overdistensions may induce barotrauma, which generally occurs regionally and may lead to air leak, pneumothorax or pneumomediastinum<sup>72</sup>. The nomenclature of barotrauma

may be misleading as the injury is caused by the exaggerated transpulmonary pressure, which may not be generated by high airway pressures only<sup>72,73</sup>. Another risk factor is the application of high tidal volumes and low positive end-expiratory pressures during mechanical ventilation, which results in volutrauma due to excessive stretch<sup>74</sup>. This phenomenon could cause alveolar and small conductive airway collapse, thereby inducing inflammation and consequent oedema<sup>75</sup>. During mechanical ventilation applying low end-expiratory lung volumes, the cyclic opening and closing of the atelectatic alveoli could damage the atelectatic and the adjacent non-atelectatic alveoli and airways by shear stress forces<sup>76</sup>. The atelectrauma phenomenon affects the surfactant function and induces regional hypoxia, thereby increase the development of pulmonary oedema<sup>77</sup>. Biotrauma is predominantly an extensive inflammatory response to mechanical lung injury. However, the possible trigger may be systemic inflammation and not only mechanically insulted lung regions<sup>78</sup>.

Ventilator-induced alveolar inflammation (Figure 2D) induces various structural and functional alterations such as epithelial-mesenchymal transformation, surfactant dysfunction, fibroproliferation, increased alveolar-capillary permeability, pulmonary oedema, overproduction of hyaline membrane and sloughing of bronchial epithelium<sup>72</sup>. These mechanisms are predominantly the consequence of different cellular processes, such as the activation and recruitment of pulmonary alveolar macrophages, activation of epithelium and endothelium along with the increase of permeability, release of mediators (tumor necrosis factor  $\alpha$ ,  $\beta$ -catenin, interleukin-6, interleukin-1 $\beta$ )<sup>79</sup>. The consequent structural and functional changes result in increased physiological dead space, decreased compliance and deteriorated gas exchange<sup>80</sup>.

## **II. AIMS AND HYPOTHESES**

The general aim of the present thesis was to investigate the respiratory consequences of untreated and treated T2DM in various ventilation scenarios. Both included studies have a randomised controlled experimental design. The first study was planned to investigate the PEEP-dependent changes of respiratory mechanics and gas exchange in the presence of untreated and metformin treated T2DM. The second study included in the present thesis investigated how treated and untreated T2DM influences the development of VILI following the application of injurious ventilation. A four-hour long ventilation scenario with high tidal volume and low PEEP allowed to assess the gas exchange and respiratory mechanical changes before, during and after VILI development. Furthermore, we aimed to characterizing the lung structural and functional changes on lung tissue samples via assessing lung injury score.

### ***II.1. Effect of T2DM on the PEEP-dependent respiratory mechanics***

The effects of T2DM separately on lung and chest wall mechanics have not been investigated yet. Furthermore, the protecting effects of metformin from respiratory consequences of diabetes remains unknown. Thus, our aim was to characterize the effects of elevated blood glucose levels on the mechanics of chest wall muscles and the lung separately at different PEEP levels. Furthermore, we investigated the related gas exchange alterations, and finally we aimed at confirming the respiratory mechanical changes with histological analysis. To address our aims, the following hypotheses were tested on the bases of theoretical considerations and previous findings:

- I. Due to the structural changes in diabetes, the end-expiratory lung volume of the animals in T2DM group may be lower than in the control animals.
- II. Since the skeletal muscles are affected by T2DM due to dycarbonil stress, their viscoelastic and mechanical properties may be compromised compared to those in the control animals.
- III. Metformin may protect the lung from adverse structural and functional changes subsequent to T2DM, thereby the respiratory mechanical and gas exchange parameters may be preserved as measured in the control animals.
- IV. The structural and functional changes in the respiratory system during diabetes can be confirmed by overexpression of collagen on lung histological samples.

## ***II.2. Modulation of VILI in models of treated and untreated T2DM***

Lung diseases or comorbidities with pulmonary manifestations facilitate acute lung injury (ALI) and acute respiratory distress syndrome (ARDS)<sup>81</sup>. Nevertheless, a potential of T2DM to protect against the development of ALI/ARDS has been reported in animal and clinical studies when sepsis was the primary cause of lung injury<sup>82</sup>. The underlying mechanisms responsible for these seemingly controversial findings are not completely clear, with the involvement of the therapeutic management of T2DM was implicated<sup>83</sup>. While a different etiology of lung injury is frequently encountered after prolonged mechanical ventilation, the effect of T2DM on the severity of VILI has not yet been characterized, and modulation potential of T2DM treatment metformin, remains unknown. Therefore, we aimed at revealing whether T2DM modulates the development of adverse respiratory symptoms of VILI by characterizing the changes in the respiratory mechanics and gas exchange parameters. Since T2DM is treated with metformin as the first-line therapy, we also aimed at exploring the potential ability of this treatment to modify VILI in T2DM with controlled hyperglycaemia.

- I. We hypothesize that following 4 hours of injurious ventilation animals with untreated T2DM will show more deteriorated gas-exchange and worse respiratory mechanics due to the adverse respiratory consequences of T2DM.
- II. Development of VILI may be protected by metformin therapy in the presence of T2DM due to the ability of such therapy to treat the adverse respiratory consequences if this metabolic disorder.
- III. The lung injury induced by prolonged mechanical ventilation may be more severe in animals with T2DM than those without metabolic disorder or in the metformin-treated diabetic animals.

### **III. MATERIALS AND METHODS**

#### ***III.1. Ethical considerations***

Both experimental protocols were part of a research project approved by the National Food Chain Safety and Animal Health Directorate of Csongrád County, Hungary (no. XXXII./150/2020) on March 18, 2020. The study procedures were implemented in compliance with the guidelines of the Scientific Committee of Animal Experimentation of the Hungarian Academy of Sciences [updated Law and Regulations on Animal Protection: 40/2013. (II. 14.), the Government of Hungary] and the European Union Directive 2010/63/EU on the protection of animals used for scientific purposes. Results were reported according to the ARRIVE guidelines<sup>84</sup>.

#### ***III.2. Pretreatments***

Both experimental protocols included in the present thesis were performed using male Wistar rats randomly assigned, at the age of 4 weeks, to one of the following three groups: untreated T2DM model (T2DM), metformin-treated T2DM model (MET), and a control group (CTRL). A well-validated T2DM model was adapted to induce diabetes in the T2DM and MET groups, which was based on feeding the animals with a special diet (HFHS U8954P Version0027, 30.3% fat, 18.4% protein, and 40.3% carbohydrate; SAFE® Plant Diets & Custom Diets, Augy, France) from the age of 5 weeks. The validity and consistency of this model to reproduce the key features of diabetes have been demonstrated in our previous study<sup>48</sup>. Rats in the CTRL group received a normal diet (A04, 3.1% fat, 16.1% protein, SAFE® Plant Diets & Custom Diets, Augy, France) before the experiments. At the age of 7 weeks, rats in the MET and T2DM groups were treated with a single low-dose intraperitoneal injection of streptozotocin (STZ, 30 mg/kg) to reduce insulin production by the pancreas, whereas rats in the CTRL group received the vehicle (citrate buffer, pH 4.4)<sup>85,86</sup>. After 4 weeks, 300 mg/kg/day metformin (Merckformin 1,000 mg, Merck, Budapest, Hungary) in drinking water was administered to rats in the MET group<sup>87,88</sup>. All rats were housed for 15 weeks before the experiments under close observation according to the animal welfare assessment and 3R guidelines.

To confirm the development of diabetes in the T2DM and MET groups, an intraperitoneal glucose tolerance test (IPGTT) was conducted 1 week after STZ or vehicle treatment to confirm the development of diabetes in the T2DM and MET groups. Baseline blood samples were collected in the morning after a 12-h overnight fast, and then 2 g/kg, 20% glucose solution was

injected intraperitoneally. Further blood samples were collected from the tail vein 30, 60, and 120 min after the glucose injection to determine the changes in blood sugar levels (Accu-Chek Active blood glucose meter; Roche, Basel, Switzerland)<sup>89,90</sup>. The area under the curve (AUC), as an indirect marker of insulin resistance, was calculated from glucose levels<sup>91</sup>. IPGTT was repeated 1 week before the experiments to confirm the development of controlled hyperglycaemia in the MET group. The standard values of the American Diabetes Association were used to define diabetes; a fasting glucose level of >7.0 mmol/L and a 120-min serum glucose level of >11.1 mmol/L were considered pathological.

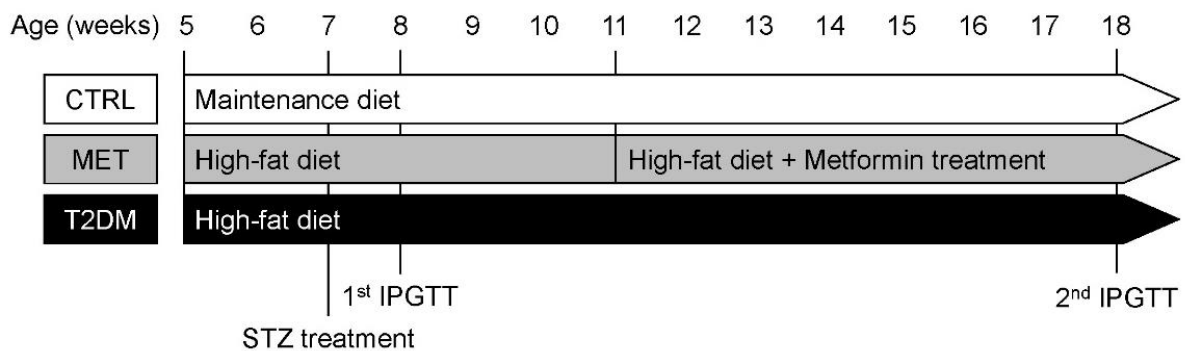


**Figure 3 Scheme of the pretreatment period**

*Abbreviations: CTRL, control group; MET, group of metformin-treated type 2 diabetic model animals; T2DM, group of untreated type 2 diabetes model rats; STZ, streptozotocin; IPGTT, intraperitoneal glucose tolerance test.*

### III.3. Group allocations and exclusions

Investigating the effect of T2DM on the PEEP-dependent respiratory mechanics, airway resistance was the primary outcome variable for estimating the sample size for repeated-measures ANOVA with a power of 0.8 and an  $\alpha$  of 0.05. Based on earlier data<sup>59</sup>, this analysis revealed that at least six animals were required in each protocol group to detect a 40% difference as statistically significant. Therefore, animals were allocated randomly to the study groups as follows: T2DM group (n=7), MET group (n=6) and CTRL group (n=7).

To describe the modulation of VILI in models of treated and untreated T2DM, PaO<sub>2</sub> was considered as the primary outcome variable to estimate sample size for repeated-measures ANOVA, with a power of 0.8 and an  $\alpha$  of 0.05. This analysis showed that at least eight animals were required in each protocol group to detect a 15% statistically significant difference in the primary outcome. To account for potential drop-out, 30 animals (ten in each protocol group) were enrolled in the present study. Two animals in the MET group were sacrificed 12 h after the STZ treatment due to their unsatisfactory health condition. Due to technical issues with

equipment and monitoring, we had to exclude one CTRL animal. We excluded three animals (two from the T2DM and one from the CTRL group) from the final analysis, due to circulatory destabilization and critical hypotension in the last period of injurious ventilation. Thus, 24 animals (CTRL, n=8; MET, n=8; T2DM, n=8) were included in the final analysis.

#### ***III.4. Animal preparations***

The anaesthesia regime and the surgical preparations were identical in the animals involved in both experimental protocols included in this the present thesis. After the 15-week long pretreatment period, rats were anesthetized via an intraperitoneal injection of sodium pentobarbital (45 mg/kg; Sigma-Aldrich, Budapest, Hungary). Under additional local anaesthesia provided by subcutaneous lidocaine (2–4 mg/kg), an 18-G cannula was inserted into the trachea via tracheostomy and then connected to a small-animal ventilator (Model 683; Harvard Apparatus, South Natick, MA). We applied volume-controlled mechanical ventilation (55–60 breaths/min, tidal volume: 7 mL/kg, with an inspired oxygen fraction of 21%). For drug administration, blood pressure measurements, and blood sample collection, the femoral artery and vein were cannulated. To maintain anaesthesia, sodium pentobarbital (5 mg/kg iv, every 30 min) was used, and muscle relaxation was provided by neuromuscular blockade with repeated intravenous administration of pipecuronium (0.1 mg/kg every 30 min; Arduan, Richter-Gedeon, Budapest, Hungary) to achieve apnoea, which was required for the mechanical measurements. Rats were placed on a heating pad with a rectal thermometer (model 507223 F; Harvard Apparatus, Holliston, MA, USA), and body temperature was maintained at  $37 \pm 0.5$  °C.

#### ***III.5. Blood gas measurements and intrapulmonary shunt fraction calculation***

In both experiments, arterial and venous blood samples (0.15 mL each) were collected simultaneously for blood gas analysis. The arterial partial pressure of oxygen ( $P_{aO_2}$ ) and arterial oxygen saturation ( $S_{aO_2}$ ) were determined using a point-of-care blood analyser system (Epoc Reader and Host; Epocal, Inc., Ottawa, ON, Canada). The capillary ( $C_{cO_2}$ ), arterial ( $C_{aO_2}$ ), and venous ( $C_{vO_2}$ ) oxygen contents were determined from the blood gas values and used to calculate the intrapulmonary shunt fraction ( $Q_s/Q_t$ ) by applying the following modified Berggren equation<sup>92</sup>:

$$\frac{Q_s}{Q_t} = \frac{C_{cO_2} - C_{aO_2}}{C_{cO_2} - C_{vO_2}}, \text{ where}$$

$$C_{aO_2} = 1.34 \times Hb_{art.} \times S_{aO_2} + P_{aO_2} \times 0.0031$$

$$CvO_2 = 1.34 \times Hb_{ven.} \times SvO_2 + PvO_2 \times 0.0031$$

$$CcO_2 = 1.34 \times Hb_{art.} \times PaO_2 \times 0.0031$$

$$PaO_2 = (FiO_2 [P_{atmos} - P_{H_2O}]) - (PaCO_2 / 0.8).$$

### III. 6. Measurement of respiratory mechanics

The forced oscillatory input impedance of the total respiratory system ( $Z_{rs}$ ) was measured using a previously described wave tube technique<sup>59</sup>. Briefly, the tracheal cannula was connected to a loudspeaker-in-box system, which generated a small-amplitude pseudorandom forcing signal (<1.5 cmH<sub>2</sub>O, with 23 noninteger multiple-frequency components between 0.5 and 20.75 Hz). During the measurement, the ventilation was suspended for a short period (8 s) at end-expiration, and the pressure oscillations were led through a wave tube (polyethylene; length 100 cm, internal diameter 2 mm). Pressure was measured simultaneously at the loudspeaker and tracheal ends of the wave tube using miniature differential pressure transducers (Honeywell Differential Pressure Sensor model 24PCEFA6D; Honeywell, Charlotte, NC).  $Z_{rs}$  was calculated as the load impedance of the wave tube<sup>93</sup>. At least four technically acceptable measurements were performed at each stage of the protocol.

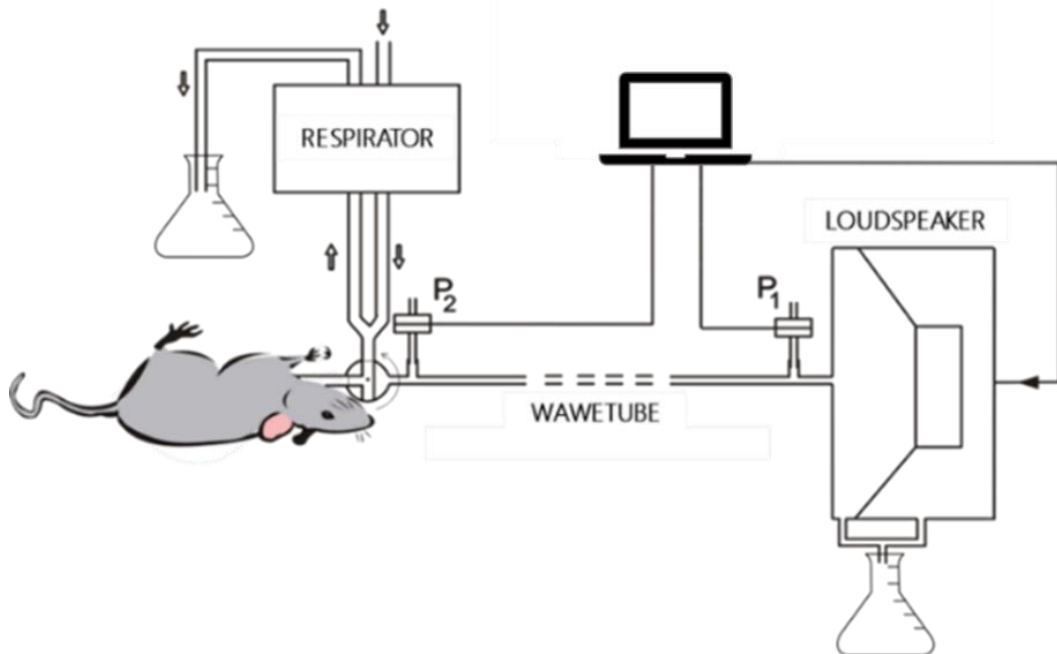


**Figure 4. Scheme of the forced oscillatory measurement apparatus**

$P_1$  and  $P_2$  indicate the miniature pressure sensors at the loudspeaker and at the tracheal end of the wave tube, respectively. During the measurements, the respiratory limb was closed, and the animal was connected to the loudspeaker via the wave tube. Between the measurements oscillatory circuit was closed and the respiratory limb was open. The Erlenmeyer flasks filled with water were used to generate PEEP.

### III.6.1. Separation of chest wall and lung mechanics

To characterize the chest wall and lung mechanical properties separately, the oesophageal pressure ( $P_{es}$ ) as a surrogate of intrapleural pressure was measured by introducing a miniature catheter-tip pressure manometer in the lower one-third of the oesophagus (SPR-524, size 2.3 F; Millar, Houston, TX). The catheter tip position was verified using the modified occlusion test for subjects under muscle relaxation<sup>94</sup>. Briefly, the airway opening was occluded, and  $P_{tr}$  and  $P_{es}$  were measured whereas gentle pressure variations were applied to the rib cage. In the absence of airflow, the positive swings of  $P_{tr}$  and  $P_{es}$  ( $\Delta P_{tr}$  vs.  $\Delta P_{es}$ ) are identical when the estimation of the overall pleural pressure by  $P_{es}$  is accurate. The mechanical impedance of the chest wall ( $Z_{cw}$ ) was determined by calculating the transfer function of  $P_{tr}$  and  $P_{es}$  as  $Z_{cw} = Z_{rs}(P_{es}/P_{tr})$ , as described previously<sup>60</sup>. For the different frequency responses of the transducers, the pressure transfer function  $P_{es}/P_{tr}$  was compensated in the frequency domain. Lung input impedance ( $Z_L$ ) was calculated as  $Z_L = Z_{rs} - Z_{cw}$ .

The mechanical properties of the lungs and the chest wall were characterized by fitting a well-validated constant-phase model to the averaged  $Z_L$  and  $Z_{cw}$  spectra by minimizing the relative difference between the measured and the modelled impedance data as follows<sup>95</sup>:

$$Z = R_N + j\omega I + (G - jH)/\omega^\alpha ,$$

where  $\alpha = (2/\pi)\arctan(H/G)$ ,  $j$  is the imaginary unit, and  $\omega$  is the angular frequency.  $R_N$  reflects the frequency-independent airway resistance when the model was fitted to  $Z_L$ , whereas it represents Newtonian (i.e., frequency-independent) resistance when model fits were performed for  $Z_{cw}$ . The parameter  $I$  is related to the inertia of the intrapulmonary gas (for  $Z_L$ ) or the chest wall tissue (for  $Z_{cw}$ ). This parameter was negligible in the frequency range studied. The viscoelastic constant-phase tissue component of the model characterizes the damping ( $G$ ) and elastic ( $H$ ) properties of the lung and chest wall compartments<sup>59,60</sup>. The tissue hysteresivity ( $\eta$ ) characterizing the coupling between the dissipative and elastic forces within the lungs and chest wall tissues, respectively, was also calculated as  $\eta = G/H$ <sup>96</sup>.

### III.6.2. Model fitting to the total respiratory impedance spectra

Due to the high tidal volumes during the injurious ventilation, reliable estimation of intrapleural pressure was not feasible. In this protocol, therefore, the mechanical properties of the total respiratory system were characterized by fitting a well-validated constant-phase model<sup>95</sup> to the

ensemble-averaged  $Z_{rs}$  spectra. The model comprises the frequency-independent airway resistance ( $R_{aw}$ ) and airway inertance in series with a viscoelastic constant-phase tissue unit that incorporates tissue damping (G) and elastance (H)<sup>95</sup>. In this case,  $G_{rs}$  and  $H_{rs}$  represents the damping and elastic properties of the total respiratory system including the lungs and the chest wall.

### ***III. 7. Lung section preparation and histological analysis***

After completion of the experimental protocols, the animals were euthanized by an overdose of pentobarbital, and midline thoracotomy was then performed. The lungs were fixed by introducing 4% paraformaldehyde through the tracheal cannula at a hydrostatic pressure of 20 cmH<sub>2</sub>O. The heart-lung block was removed in one piece from the thoracic cavity and stored in 4% paraformaldehyde at 4°C overnight and then in phosphate-buffered saline. A 5- $\mu$ m thick region was embedded from the subhilar region of the left lung and three 7- $\mu$ m thick sections were cut from each lung using a microtome (Leica RM2521 RTS, Leica Microsystems GmbH, Wetzlar, Germany). A 35- $\mu$ m space (5 sections) was discarded between each analysed 7- $\mu$ m thick section.

#### *III.7.1. Effect of T2DM on the PEEP-dependent respiratory mechanics*

To quantify the collagen in the lungs, Masson's trichrome staining was performed (Trichrome Stain Kit, ab150686, Abcam, Cambridge, UK) according to the manufacturer's instructions. At least two representative rectangular fields were digitalized from each section using a Nikon-DS Fi3 camera attached to a Leica DM 2000 Led light microscope (Leica Microsystems GmbH, Germany) at  $\times 400$  magnification. Fields contained alveoli without bronchi or large vessels. The collagen was segmented and quantified using the Trainable Weka Segmentation plugin in ImageJ software (Wayne Rasband, NIH, Bethesda, MD, USA). Collagen area was expressed as a percentage of collagen deposits referred to the lung total area. To determine an index for the overall alveolar diameters, the mean linear intercept was calculated by using a well-established protocol for ImageJ<sup>97</sup>. The histological analyses were made by one trained person who was blinded to the group allocation.

#### *III.7.2. Modulation of VILI in models of treated and untreated T2DM*

The lung injury was determined by observing the sections stained with haematoxylin and eosin under a light microscope. Each slide was evaluated by three separate investigators in a blinded manner. To calculate the lung injury score (LIS), a total of 25 alveoli were counted in each field

at  $\times 400$  magnification. Points were assigned according to previously established criteria. LIS was calculated using the following formula:  $LIS = [(alveolar\ haemorrhage\ points) + 2 \times (alveolar\ infiltrate\ points) + 3 \times (fibrin\ points) + (alveolar\ septal\ congestion\ points)] / total\ number\ of\ alveoli\ counted\ in\ the\ field^{98}$ . To evaluate oxidative DNA damage, sections were selected for the permanent immunocytochemical staining of 8-hydroxy-2'-deoxyguanosine (8-OHDG). After routine deparaffinization, heat-induced antigen retrieval was performed by immersing the slides in 0.01M sodium citrate buffer (pH 6.0). Endogenous peroxidases were blocked using 5%  $H_2O_2$ . Nonspecific protein-binding sites were blocked using 5% normal goat serum (Merck, Kenilworth, NJ, United States), and the sections were permeabilized with 0.5% Triton X-100 (Merck, Kenilworth, NJ, United States) in Tris-buffered saline. The sections were incubated overnight with mouse monoclonal anti-8-OHDG (Abcam, ab48508, 1:200) at 4°C. The subsequent steps of incubation consisted of an enhancer reagent at room temperature for 1 h and horseradish-peroxidase linked secondary antibody also at room temperature for 3 h. These are the components of the Polink-2 Plus HRP Detection Kit (for mouse primary antibody with diaminobenzidine (DAB) chromogen, D37-18, GBI Labs, Bothell, WA, USA). Positivity to 8-OHDG was visualized with DAB, and the sections were overstained with haematoxylin<sup>99</sup>. On each section, nine fields were digitally recorded using a Nikon-DS Fi3 camera attached to a Leica DM 2,000 Led light microscope (Leica Microsystems GmbH, Wetzlar, Germany) at  $\times 200$  magnification. Fields were evaluated by manual cell counting using the Cell Counter plugin of ImageJ (Wayne Rasband, NIH, Bethesda, MD, USA) by two observers blinded to the experimental design<sup>100</sup>.

### ***III. 8. Additional measurements***

#### ***III.8.1. Thoracic gas volume***

To determine the alterations of end-expiratory lung volumes in the presence of diabetes, following the surgical preparations the tracheotomized and mechanically ventilated rats were placed into a whole-body plethysmograph. The trachea and box were closed at end-expiration, and then the pressure in the trachea and box was measured while the animal made spontaneous breathing efforts against the closed trachea (5–15 s). Measurements were performed at PEEP of 0, 3, and 6 cmH<sub>2</sub>O (PEEP 0, 3, and 6) to assess the alterations in lung collapsibility by T2DM and its potential prevention by metformin treatment. The thoracic gas volume (TGV) was calculated from the simultaneously measured pressure signals by applying the Boyle–Mariotte

law. To compensate for differences in body size among the animals, TGV was normalized to bodymass ( $nTGV = TGV/bodymass$ )<sup>101</sup>.

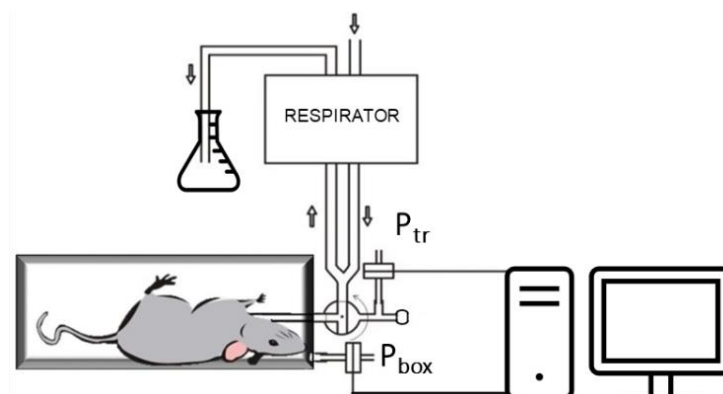


**Figure 5. Scheme of the measurement setup for the assessment of thoracic gas volume**  
Abbreviations:  $P_{tr}$ , trachea pressure;  $P_{box}$ , plethysmography box pressure.

### III.9. Experimental protocols

#### III.9.1. Effect of T2DM on the PEEP-dependent respiratory mechanics

Following the pretreatment period, the animals were anesthetized, tracheostomy was performed, and mechanical ventilation was initiated as detailed above. TGV was then measured at PEEP levels of 0, 3, and 6 cmH<sub>2</sub>O using a whole-body plethysmograph. The intraoesophageal catheter was then introduced to measure  $P_{es}$ , and its position was verified using the modified occlusion test. The animals were then ventilated while maintaining PEEP of 3 cmH<sub>2</sub>O, and a hyperinflation manoeuvre was performed by closing the expiratory limb of the ventilator tubing until the next expiration to standardize the volume history. After 3 min, arterial and venous blood gas samples were taken simultaneously, and the first set of lung and chest wall mechanical impedance data was collected. Following a 5-min adaptation period, blood gas analyses and forced oscillatory data recordings were repeated under PEEP levels of 0 and 6 cmH<sub>2</sub>O in random order. Electrocardiogram and systemic blood pressure were registered continuously during the whole protocol (Biopac, Goleta, CA, USA) At the end of the measurements, the animals were euthanized by an overdose of sodium pentobarbital (200 mg/kg), and the lungs were excised for histological analysis.



**Figure 6. Protocol scheme: Effect of T2DM on the PEEP-dependent respiratory mechanics**

*Abbreviations: TGV, thoracic gas volume assessments; BG, blood gas analysis; FOT, forced oscillation measurements.*

### *III.9.2. Modulation of VILI in models of treated and untreated T2DM*

After the pretreatment period, the rats were anesthetized and ventilated in the volume control mode with physiological parameters (VT: 7 mL/kg, PEEP: 3 cmH<sub>2</sub>O and 55–60/min frequency) for 20 min. Airway opening pressure was monitored to evaluate the peak inspiratory pressure (PIP), and electrocardiogram and systemic blood pressure were also registered (Biopac, Goleta, CA, USA). Next, forced oscillatory measurements were performed to evaluate the respiratory mechanics, and then arterial and venous blood samples were collected for blood gas analyses. An injurious ventilation strategy was initiated to induce VILI by setting high VT (23 mL/kg) and low PEEP (0 cmH<sub>2</sub>O), and it was maintained for 4 h. To avoid severe hypocapnia, the ventilation frequency was reduced to 25–30/min to maintain minute ventilation and the end-tidal CO<sub>2</sub> in the range of 25–30 mmHg. This ventilation has been demonstrated to induce VILI consistently by the simultaneous induction of barotrauma due to the high VT and atelectrauma as a consequence of low PEEP<sup>102</sup>. Forced oscillatory measurement of the respiratory mechanics and blood gas analyses were conducted after a 15-min period that was allowed for the stabilization of respiratory and hemodynamic variables (0 h) and 2 and 4 h after the onset of injurious ventilation. After the completion of the measurement protocol, the animals were euthanized by an overdose of pentobarbital (200 mg/kg), and the lungs were removed for histological analysis, as detailed earlier.

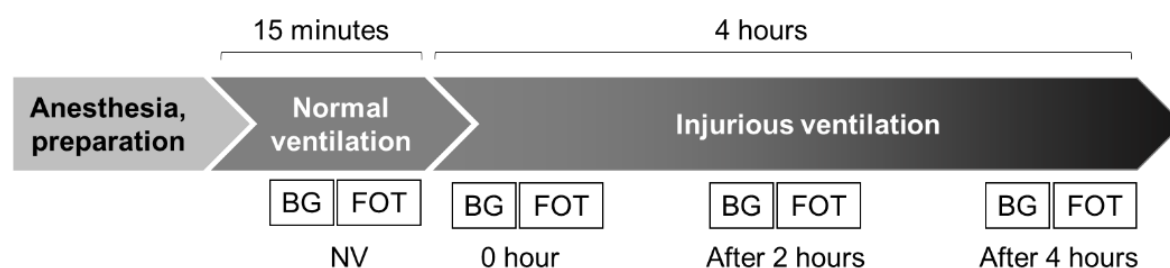


**Figure 7. Protocol scheme: Modulation of VILI in models of treated and untreated T2DM**  
*Abbreviations: NV, volume-controlled ventilation with physiological parameters; BG, blood gas analysis; FOT, forced oscillation measurements.*

### *III.10. Statistical analysis*

Data are expressed as the means  $\pm$  standard deviation for normally distributed variables or boxplots to demonstrate the median and interquartile range in cases of a lack of normality. To

evaluate data distributions for normality, the Shapiro–Wilk test was used. Statistical analyses were conducted with a significance level of  $p < 0.05$ , and all reported  $p$  values are two-tailed.

### *III.10.1. Effect of T2DM on the PEEP-dependent respiratory mechanics*

Two-way repeated-measures ANOVA with Holm–Šidák *post hoc* analyses was used to test the effects of diabetes and metformin therapy on the PEEP-dependent changes of respiratory mechanical and oxygenation parameters. One-way ANOVA with Holm–Šidák *post hoc* tests was applied to assess significant differences in the AUC of IPGTT and histological outcomes between the protocol groups.

### *III.10.2. Modulation of VILI in models of treated and untreated T2DM*

Two-way repeated-measures ANOVA with Holm–Šidák *post hoc* analyses was used to explore the effects of diabetes induction and metformin therapy. One-way ANOVA with Holm–Šidák *post hoc* tests were applied to determine the differences in body weights and the AUC values of IPGTT and in the histological outcomes between the protocol groups. The oxygenation and respiratory mechanical parameters are represented either as absolute values, where two-way repeated-measures ANOVA with Holm–Šidák *post hoc* analyses was used to determine the changes during the injurious ventilation, or as relative values (difference between 0 and 4 h), where one-way ANOVA with the Holm–Šidák method was used.

## IV. RESULTS

### IV.1. Effect of T2DM on the PEEP-dependent respiratory mechanics

#### IV.1.1. Body weights and results of IPGTTs

No significant difference in body mass was observed between the CTRL ( $454 \pm 36$  g) and T2DM groups ( $451 \pm 45$  g), whereas bodymass was significantly lower in the MET group ( $409 \pm 36$  g,  $p < 0.05$ ).

The first IPGTT performed following 1 week of STZ or vehicle treatment and 4 weeks of special diet feeding resulted in mean fasting glucose levels below the threshold level of 7.0 mmol/L in the CTRL group ( $5.2 \pm 0.5$  mmol/L), whereas mean fasting glucose levels tended to be elevated in the T2DM and MET groups ( $7.4 \pm 0.9$  and  $7.5 \pm 0.7$  mmol/L, respectively). The second IPGTT revealed normal fasting serum glucose levels in the CTRL group ( $6.0 \pm 0.6$  mmol/L), whereas prolonged high-fat diet feeding and STZ treatment resulted in marked elevation in this parameter in the rats of group T2DM ( $9.7 \pm 1.0$  mmol/L). A diminished fasting serum glucose level was observed in the MET group ( $7.0 \pm 1.1$  mmol/L).

During the first IPGTT, the AUCs were significantly higher in the T2DM and MET groups than in the CTRL group (both  $p < 0.001$ ). The second IPGTT revealed no significant change in the AUC in the CTRL group, whereas further marked and significant elevation of the AUC was observed in the T2DM group ( $p < 0.001$ ). Meanwhile, the AUC in the MET group was intermediate ( $p < 0.001$ ).

	First IPGTT	Second IPGTT
<b>Group CTRL</b>	$14.6 \pm 1.6$	$18.0 \pm 2.3$
<b>Group MET</b>	$35.3 \pm 4.8^{\$}$	$27.6 \pm 3.9^{*\$}$
<b>Group T2DM</b>	$33.2 \pm 7.9^{\$}$	$47.4 \pm 4.7^{*\$}$

**Table 1. AUCs of the first and second IPGTT**

The area under the curve (AUC) values as a marker of insulin resistance obtained from the first and second intraperitoneal glucose tolerance tests (IPGTT). \*:  $p < 0.05$  vs. first IPGTT; \$:  $p < 0.05$  vs. CTRL; §:  $p < 0.05$  vs. MET. Abbreviations: CTRL, control group ( $n=7$ ); MET, group of metformin-treated type 2 diabetic model animals ( $n=6$ ); T2DM, group of untreated type 2 diabetic model rats ( $n=7$ ).

#### IV.1.2. Thoracic gas volumes

Table 2 presents nTGV in the protocol groups at each PEEP level. Whereas nTGV significantly increased with increasing PEEP ( $p < 0.001$ ), no significant differences were observed among the study groups at any PEEP.

	<b>PEEP 0</b> (ml/kg)	<b>PEEP 3</b> (ml/kg)	<b>PEEP 6</b> (ml/kg)
<b>Group CTRL</b>	7.29 ± 1.51	11.85 ± 3.41*	16.69 ± 5.70*#
<b>Group MET</b>	7.36 ± 1.53	11.53.6 ± 2.15*	19.62 ± 5.44*#
<b>Group T2DM</b>	8.75 ± 1.71	14.19 ± 3.56*	20.18 ± 4.67*#

**Table 2. The thoracic gas volume normalized to the body mass**

Normalized thoracic gas volume (nTGV) obtained by whole body plethysmography in the study groups at positive end-expiratory levels of 0, 3 and 6 cmH<sub>2</sub>O (PEEP 0, PEEP 3, PEEP 6). \*:  $p < 0.001$  vs. PEEP 0; #:  $p < 0.001$  vs PEEP 3. Abbreviations: CTRL, control group ( $n=7$ ); MET, group of metformin-treated type 2 diabetic model animals ( $n=6$ ); T2DM, group of untreated type 2 diabetic model rats ( $n=7$ ).

#### IV.1.3. Mechanical impedance data and model fitting performance

Mechanical impedance spectra in a representative rat for the  $Z_{rs}$ ,  $Z_L$  and  $Z_{cw}$ , at three different PEEP levels (0-3-6 cmH<sub>2</sub>O) demonstrated on Figure 8.

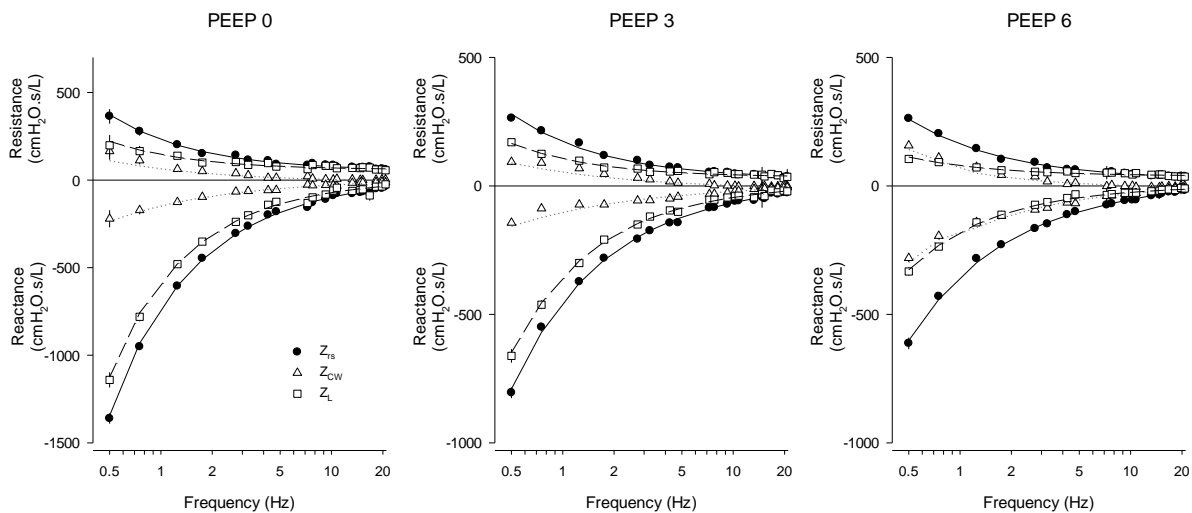


**Figure 8. Mechanical impedance spectra in a representative rat**

Resistance (real part, top) and reactance (imaginary part, bottom) of the input impedance of the total respiratory system ( $Z_{rs}$ , filled circles) and its main compartments, the lungs ( $Z_L$ , open squares) and the chest wall ( $Z_{cw}$ , open triangles), obtained in a representative rat at 0 (left), 3 (middle) and 6 cmH<sub>2</sub>O PEEP levels (right). For simplicity, impedance data included in the model fits are displayed with the corresponding model fits to  $Z_{rs}$  (continuous lines),  $Z_L$  (broken lines), and  $Z_{cw}$  (dotted lines).

The fitting performance of the constant-phase model is summarized on Table 3.

		<b>CTRL</b>	<b>MET</b>	<b>T2DM</b>
<b>PEEP 0</b>	<b>Z<sub>rs</sub></b>	7.07 ± 2.69 %	6.79 ± 2.56 %	6.14 ± 2.92 %
	<b>Z<sub>L</sub></b>	9.62 ± 5.08 %	7.83 ± 3.07 %	8.59 ± 3.72 %
	<b>Z<sub>cw</sub></b>	10.37 ± 4.78 %	10.41 ± 4.2 %	8.34 ± 1.28 %
<b>PEEP 3</b>	<b>Z<sub>rs</sub></b>	8.19 ± 1.43 %	6.19 ± 1.89 %	6.83 ± 1.47 %
	<b>Z<sub>L</sub></b>	6.84 ± 3.21 %	5.71 ± 1.08 %	7.68 ± 3.02 %
	<b>Z<sub>cw</sub></b>	7.82 ± 0.64 %	6.70 ± 2.11 %	7.09 ± 0.49 %
<b>PEEP 6</b>	<b>Z<sub>rs</sub></b>	6.64 ± 1.35 %	7.30 ± 1.74 %	9.01 ± 3.27 %
	<b>Z<sub>L</sub></b>	8.75 ± 6.15 %	6.62 ± 1.70 %	9.44 ± 5.89 %
	<b>Z<sub>cw</sub></b>	8.46 ± 4.65 %	7.11 ± 2.38 %	7.19 ± 0.34 %

**Table 3. Fitting errors**

*Fitting errors in the three protocol groups at different PEEP levels (0-3-6 cmH<sub>2</sub>O) respectively for the input impedance of the total respiratory system (Z<sub>rs</sub>), the lungs (Z<sub>L</sub>) and the chest wall (Z<sub>cw</sub>). Abbreviations: CTRL, control group (circles, n=7); MET, metformin-treated model of type 2 diabetes (squares, n=6); T2DM, untreated model of type 2 diabetes (triangles, n=7). Two-way repeated-measures ANOVA with Holm–Šidák post hoc analyses was used to test the between-group and within-group differences; statistically significant difference was not observed between protocol groups (CTRL-MET-T2DM) or compartments (Z<sub>rs</sub>-Z<sub>L</sub>-Z<sub>cw</sub>).*

#### IV.1.4. Lung and chest wall mechanical parameters

Elevation of PEEP resulted in significant decreases in the pulmonary components of R<sub>N</sub>, G, and H (all p < 0.05), whereas mechanical parameters representing the chest wall mechanics were less affected by PEEP changes (Figure 9). The between-group differences in R<sub>N</sub>, G, and H of the lungs were significantly larger at PEEP 0 in the T2DM group than in the other groups, whereas η was significantly smaller (all p < 0.05). These differences among the protocol groups were not detectable at higher PEEP levels. No significant difference was evidenced among the protocol groups in R<sub>N</sub>, G, and H of the chest wall. Conversely, chest wall η was significantly lower in the T2DM group than in the CTRL group at PEEP 0 (p < 0.05).

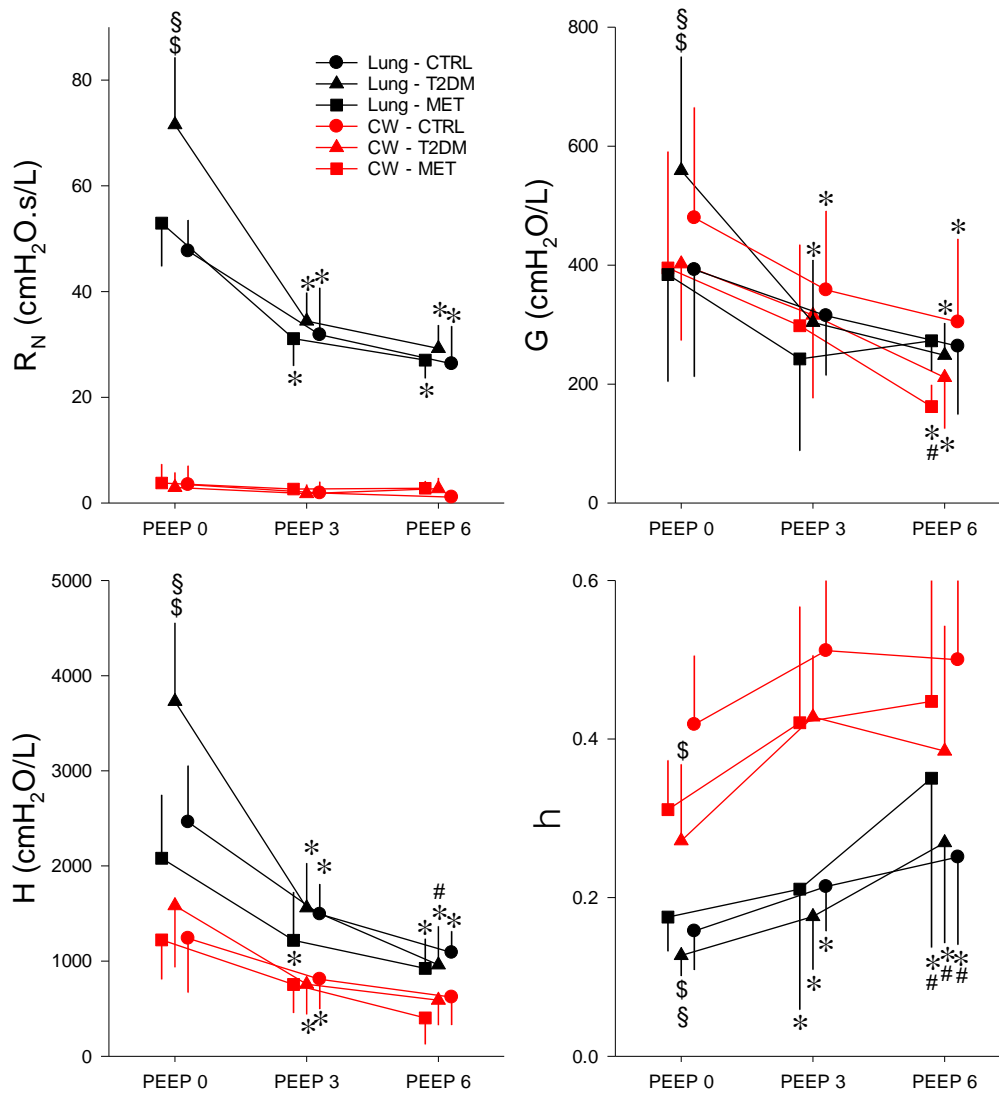


**Figure 9. Lung and chest wall mechanical parameters at different PEEP levels**

Mechanical parameters characterizing the lungs (black) and the chest wall (red) at PEEP levels of 0, 3, and 6 cmH<sub>2</sub>O (PEEP 0, PEEP 3, and PEEP 6, respectively). Abbreviations: CTRL, control group (circles, n=7); MET, metformin-treated model of type 2 diabetes (squares, n=6); T2DM, untreated model of type 2 diabetes (triangles, n=7); R<sub>N</sub>, Newtonian resistance; G, tissue damping; H, tissue elastance; η, hysteresivity (G/H). \$: p < 0.05 vs. CTRL within a specific PEEP level; §: p < 0.05 vs. MET within a specific PEEP level; \*: p < 0.05 vs. PEEP 0 within the same group; #: p < 0.05 vs. PEEP 3 within the same group.

#### IV.1.5. Gas exchange parameters

As demonstrated on Figure 10, Qs/Qt was significantly higher and SaO<sub>2</sub> was significantly lower in the T2DM group than in the MET and CTRL groups at PEEP 0 and 6 (all p < 0.001). At PEEP 0, a significant decrease of PaO<sub>2</sub> was observed in the T2DM group compared to those in the CTRL and MET groups (p < 0.001 and p < 0.05, respectively), whereas these differences were not statistically detectable at higher PEEP levels.

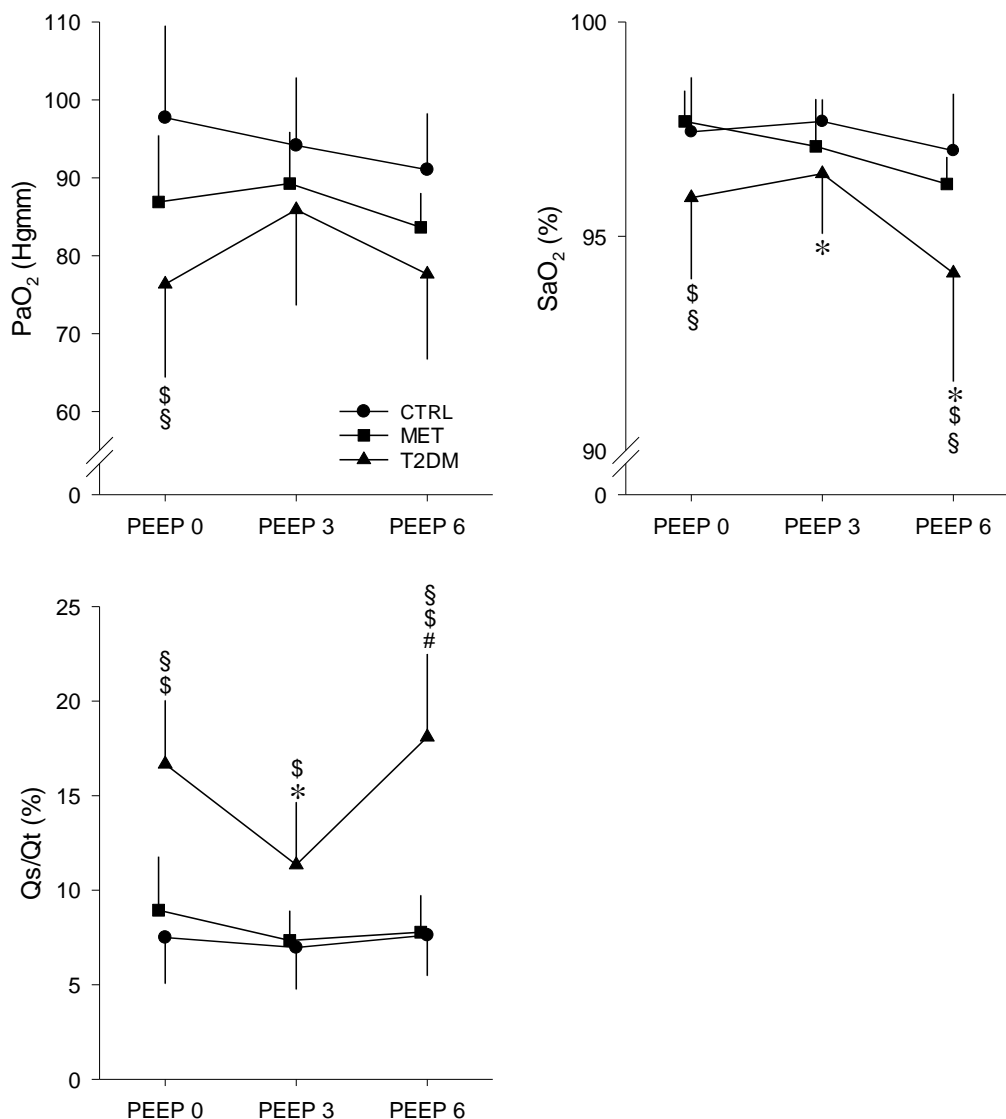


**Figure 10. Gas-exchange parameters obtained at different PEEP levels**

Gas-exchange parameters obtained at positive end-expiratory pressure levels of 0, 3 and 6 cmH<sub>2</sub>O (PEEP 0, PEEP 3, and PEEP 6, respectively). Abbreviations: CTRL, control group (circles); MET, metformin-treated model of type 2 diabetes (squares); T2DM, untreated model of type 2 diabetes (triangles); PaO<sub>2</sub>, arterial partial pressure of oxygen; SaO<sub>2</sub>, arterial oxygen saturation; Qs/Qt, intrapulmonary shunt fraction. \$:  $p < 0.05$  vs. CTRL within the same PEEP level; §:  $p < 0.05$  vs. MET within the same PEEP level; \*:  $p < 0.05$  vs. PEEP 0 within the same group; #:  $p < 0.05$  vs. PEEP 3 within the same group.

#### IV.1.6. Haemodynamics

While significant decrease in the mean arterial pressure (MAP) was observed in Group CTRL when PEEP was elevated from 0 to 6 cmH<sub>2</sub>O ( $-124 \pm 155\%$ ), rats in the Groups T2DM or MET exhibited no significant change in MAP with increasing PEEP ( $-2.8 \pm 10.6\%$  and  $-26 \pm 32\%$ , respectively).

#### IV.1.7. Lung histological findings

Figure 11 demonstrates the mean linear intercept and differences in collagen expression obtained by histology in the three protocol groups. While the mean linear intercept did not show any difference between the protocol groups, the percentage area of collagen deposition in the lung parenchyma was significantly higher in the MET and T2DM groups than in the CTRL group (both  $p < 0.001$ ). Furthermore, significant overexpression of collagen was also apparent in the T2DM group compared to its expression in the MET group ( $p < 0.001$ ).

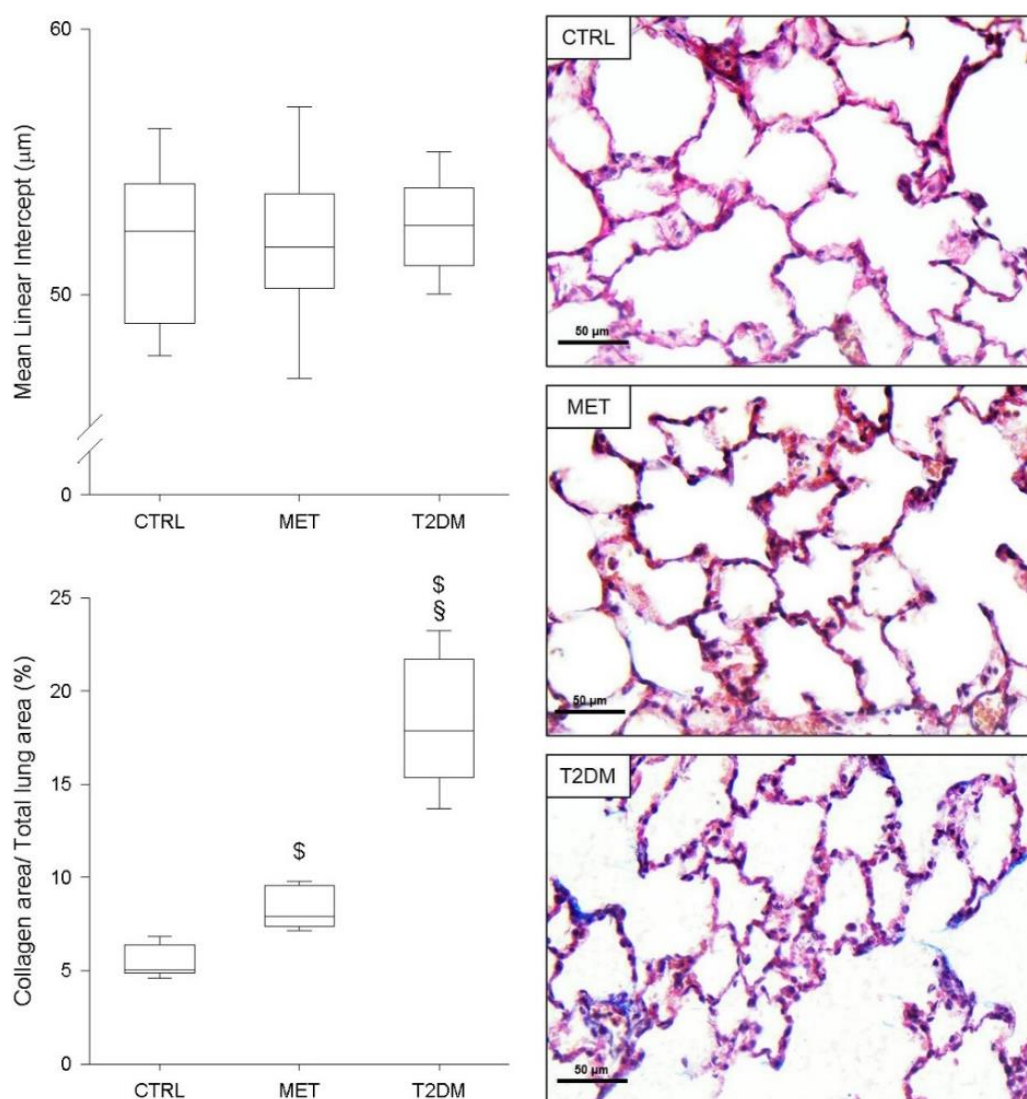


**Figure 11. Mean linear intercept and differences in collagen expression in lung tissue**  
Mean linear intercept as an indicator of mean alveolar diameter and collagen area as a percentage of total lung tissue area with representative histological images of lung sections stained with Masson's trichrome in the study groups (magnification,  $\times 400$ ; scale bar,  $50 \mu\text{m}$ ). Abbreviations: CTRL, control group; MET, metformin-treated model of type 2 diabetes; T2DM, untreated model of type 2 diabetes;  $\$$ :  $p < 0.05$  vs. CTRL;  $\S$ :  $p < 0.05$  vs. MET.

## IV.2. Modulation of VILI in models of treated and untreated T2DM

### IV.2.1. Results of IPGTTs

The serum glucose levels and the corresponding AUC values during IPGTTs are summarized in Figure 12. At the first IPGTT mean fasting glucose level in the CTRL group was below the threshold level of 7.0 mmol/l, but it reached or exceeded this level in the other two groups, furthermore the registered values were significantly higher both diabetic groups ( $7.7 \pm 1.3$  mmol/L and  $7.4 \pm 0.8$  mmol/L, respectively) compared to the animals of the CTRL group ( $5.2 \pm 0.4$  mmol/L,  $p < 0.05$  for both). In the measurement performed at 120 min, the mean glucose level in the CTRL group ( $6.4 \pm 0.9$  mmol/L) was below 11.1 mmol/l, but it has exceeded this critical level in the MET and T2DM groups ( $16.2 \pm 3.1$  mmol/L;  $13.4 \pm 4.2$  mmol/L). This difference between the groups was statistically significant ( $p < 0.01$ ). During the second IPGTT, the fasting glucose levels of the CTRL group ( $6.1 \pm 0.6$  mmol/L) was in the normal range, but the values of MET and T2DM animals ( $7.1 \pm 4.2$  mmol/L and  $9.6 \pm 0.9$  mmol/L, respectively) were over the threshold level of 7.0 mmol/L. At 120-min measurements the blood glucose levels of T2DM group were significantly higher than those in the MET and CTRL groups ( $26.2 \pm 4.1$  mmol/L vs  $13.1 \pm 2.5$  mmol/L and  $7.8 \pm 1.4$  mmol/L  $p < 0.001$ , respectively). The AUC values were significantly increased in the T2DM group ( $p < 0.001$ ) and decreased in the MET group ( $p < 0.001$ ). During the 1st IPGTT, the AUC values were significantly higher in groups with diabetes. Although this difference was detected during the 2nd IPGTT ( $p < 0.001$ ), the AUC value in the T2DM group was higher than that in the MET group ( $p < 0.001$ ).

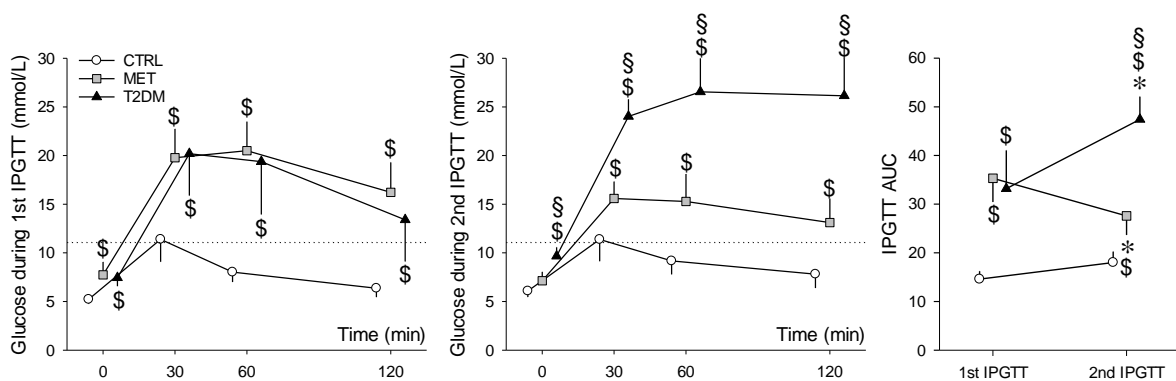


**Figure 12. Serum glucose levels and the corresponding AUC values during IPGTTs**  
 Blood glucose levels and the corresponding (under curve area) AUC values belonging to the 1st and 2nd IPGTT measurements during the pretreatment period. \*:  $p < 0.05$  vs. 1st IPGTT; \$:  $p < 0.05$  vs. CTRL; §:  $p < 0.05$  vs. MET. Abbreviations: CTRL, control group; MET, metformin-treated model of type 2 diabetes; T2DM, untreated model of type 2 diabetes; IPGTT,

*intraperitoneal glucose tolerance test. Dotted line denotes the threshold glucose levels for 120-minutes blood glucose measurements (11.1 mmol/L).*

### VI.2.2. Gas exchange parameters

Figure 13 shows the gas exchange parameters during normal ventilation (NV) and after injurious ventilation (0–4 h) in the study groups. Although  $\text{PaO}_2$  decreased in the CTRL group after 4 h of injurious ventilation ( $p < 0.05$ ), this decline was more significantly manifested in the T2DM group ( $p < 0.001$ ). Rats in the MET and CTRL groups demonstrated only tendencies for worsening in  $\text{SaO}_2$  and  $Q_s/Q_t$ , whereas rats in the T2DM group exhibited significantly compromised gas exchange due to injurious ventilation ( $p < 0.05$ ). When the alterations in gas exchange indices were expressed as relative changes compared with the onset of injurious ventilation (0 h), significantly greater deterioration was observed in  $\text{PaO}_2$  and  $\text{SaO}_2$  in the T2DM group than in the other two groups ( $p < 0.05$ ).

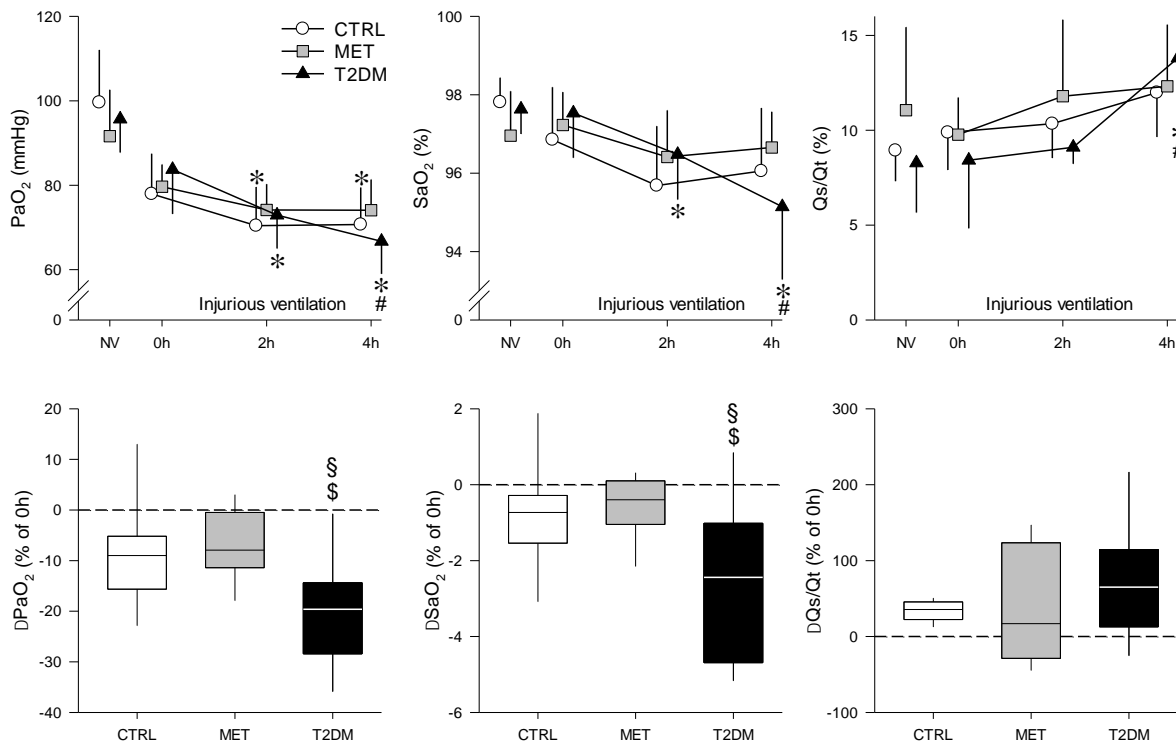


**Figure 13. Gas exchange parameters during normal- and after injurious ventilation**  
 Partial oxygen pressure ( $\text{PaO}_2$ ) and oxygen saturation ( $\text{SaO}_2$ ) of the arterial blood and the intrapulmonary shunt fraction ( $Q_s/Q_t$ ) obtained during volume-controlled ventilation with physiological parameters (NV) and injurious ventilation in control rats (CTRL), in rats with metformin-treated type 2 diabetes (MET), and in rats with untreated type 2 diabetes (T2DM). Upper panels: Absolute changes in mean values  $\pm$  standard deviation (SD). Lower panels: Changes after 4 h of injurious ventilation values relative to the values obtained at 0 h. \*:  $p < 0.05$  vs. 0 h; #:  $p < 0.05$  vs. 2 h; \$:  $p < 0.05$  vs. CTRL; §:  $p < 0.05$  vs. MET.

### IV.2.3. Respiratory mechanical alterations

Figure 14 depicts the changes in PIP and the airway and respiratory tissue parameters obtained during NV and injurious ventilation (0–4 h). Significantly higher PIP was recorded in the T2DM group than in the other study groups throughout the study period ( $p < 0.05$ ), and the rats in the T2DM group exhibited significant increases in PIP after 4 h of injurious ventilation ( $p < 0.05$ ). Rats in the T2DM group also showed higher Raw values than those in the CTRL group at the onset of injurious ventilation (0 h,  $p = 0.013$ ). This difference was also observed after 4 h of injurious ventilation ( $p = 0.012$ ), with significance also being detected in comparison with the MET group ( $p < 0.05$ ). Respiratory tissue mechanical parameters exhibited no significant difference between the study groups at any time point of measurement.

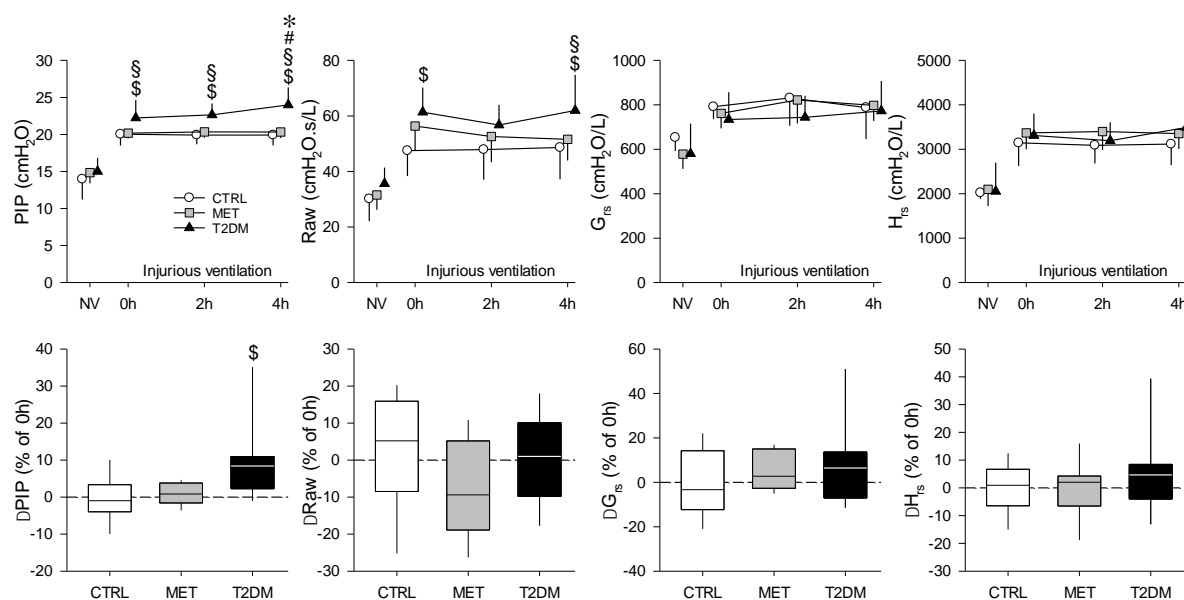


**Figure 14. Respiratory mechanics obtained during normal- and injurious ventilation**  
Peak inspiratory pressure (PIP), airway and viscoelastic respiratory tissue mechanical parameters obtained during volume-controlled ventilation with physiological parameters (NV) and injurious ventilation in control rats (CTRL), in rats with metformin-treated type 2 diabetes (MET), and in rats with untreated type 2 diabetes (T2DM). Upper panels: Absolute changes in mean values  $\pm$  standard deviation (SD). Lower panels: Changes after 4 h of injurious ventilation values relative to the values obtained at 0 h. \*:  $p < 0.05$  vs. 0 h; #:  $p < 0.05$  vs. 2 h; \$:  $p < 0.05$  vs. CTRL; §:  $p < 0.05$  vs. MET. Abbreviations: Raw, airway resistance; G, tissue damping (resistance); H, tissue elastance.

### IV.2.4. Lung injury score – results of histological analysis

Figure 15 summarizes the histological findings related to the different injury types. LIS was significantly higher in the T2DM group than in the CTRL and MET groups ( $p < 0.001$ ). The grades of intra-alveolar fibrin were significantly higher in the T2DM than in the CTRL group

( $p = 0.018$ ), and the grades of intra-alveolar infiltrates were significantly higher in the T2DM group than in the MET group ( $p = 0.009$ ), the alveolar septal congestion and alveolar hemorrhage were significantly more intense in the T2DM group than in both CTRL and MET groups ( $p < 0.001$ ).

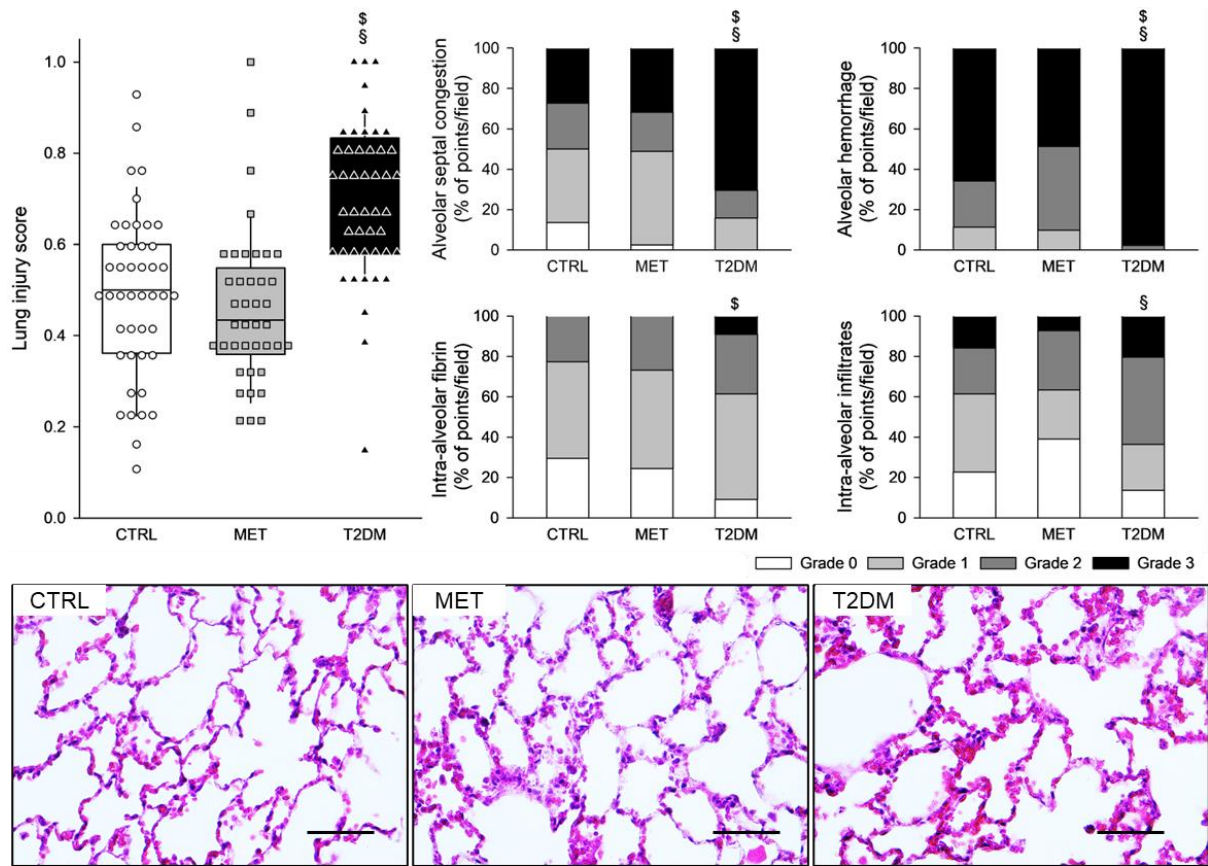


**Figure 15. Lung injury scores and representative images**

Lung injury score (LIS) in control rats (CTRL), in rats with metformin-treated type 2 diabetes (MET), and in rats with untreated type 2 diabetes (T2DM) and its components describing the different types of lung injuries. Each symbol represents the LIS value on a field of view. Representative images of lung sections stained with hematoxylin and eosin are also demonstrated (magnification  $\times 400$ ; scale bar: 50  $\mu\text{m}$ ).  $\$$ :  $p < 0.05$  vs. CTRL;  $\S$ :  $p < 0.05$  vs. MET.

#### IV.2.5. Number of 8-OHDG positive cells – results of immunohistochemistry

The number of anti-8-OHDG-positive-stained nuclei is presented in Figure 16. Rats in the MET group exhibited significantly higher number of positive-stained nuclei than those in the CTRL group ( $p = 0.037$ ), whereas the number of positive-stained nuclei in the lungs of T2DM rats was significantly greater than that in both CTRL and MET rats ( $p < 0.001$ ).

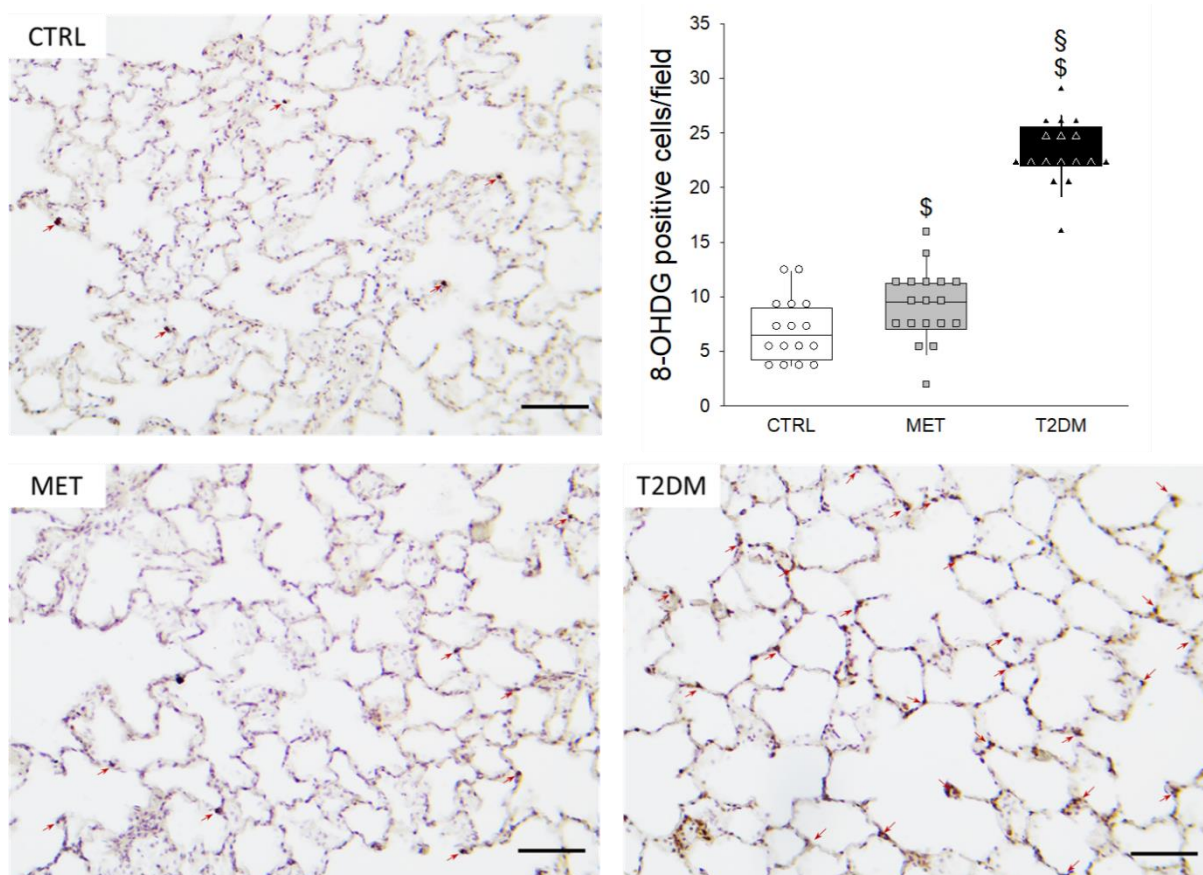


**Figure 16. Number of 8-OHDG positive cells and representative images**

Representative lung sections of the three study groups stained with anti-8-OHDG immunohistochemistry. Red arrows indicate the 8-OHDG-positive cells (magnification  $\times 200$ ; scale bar:  $100 \mu\text{m}$ ). Abbreviations: CTRL, control group; MET, metformin-treated model of type 2 diabetes; T2DM, untreated model of type 2 diabetes. Graph represents the number of anti-8-OHDG positive-stained cells in the three study groups. \$:  $p < 0.05$  vs. CTRL; §:  $p < 0.05$  vs. MET.

## V. DISCUSSION

The chronic hyperglycemia in T2DM affects various organ systems and biological processes due to alterations in molecular mechanisms, cell, and tissue functions. The environmental and genetic factors, which are responsible for the development of T2DM often increase the risk of comorbidities such as obesity, hypertension, atherosclerosis *etc.* These etiopathologies also lead to a systemic inflammation which potentially affects the respiratory system. Although, several studies attempted to investigate the respiratory consequences of T2DM, the exact mechanisms and the response of the diabetic lung to various ventilation settings are unclear. Furthermore, the studies about T2DM regularly use pure diabetes models, without treatment factors such as metformin therapy, however, our diabetic patients typically live with controlled hyperglycemia due to certain antidiabetic medications. The respiratory alterations of treated and untreated T2DM model were investigated during the application of different ventilation scenarios. Using different PEEPs and an injurious ventilation protocol, we studied the alterations of respiratory mechanics and gas exchange in well-established rodent models of untreated and metformin-treated T2DM.

### *V.1. Effect of T2DM on the PEEP-dependent respiratory mechanics*

Separate assessment of the mechanical properties of the lungs and chest wall in an experimental model of type 2 diabetes revealed the involvement of both compartments in the detrimental changes in global respiratory mechanics. At low PEEP, diabetes elevated mechanical parameters reflecting airflow and lung tissue resistance and stiffness of the pulmonary parenchyma. Increasing lung volume alleviated these pulmonary mechanical abnormalities. Regarding the effect of sustained hyperglycaemia on the chest wall, only tendencies of changes in the dissipative or elastic properties of chest tissues were observed. However,  $\eta$  reflecting the coupling of these mechanical properties was disturbed at low PEEP with a shift toward the dominance of elastic forces. Although metformin-treated diabetic animals displayed no signs of abnormal lung or chest wall mechanics, gas exchange defects or the remodelling of the extracellular fibre network was observed in the lung connective tissue in histopathological examinations.

To induce T2DM, a well-established model was created by administering a single low dose of STZ combined with high-fat diet feeding<sup>48,86</sup>. The beta cell-damaging agent STZ induces necrosis followed by atrophy of the Langerhans islets. According to the diagnostic criteria, rats in both the T2DM and MET groups exhibited definitive blood glucose parameters characteristic

of diabetes during the first IPGTT, performed before the initiation of metformin therapy (Table 1). The mode of administration and the daily dose of metformin were adapted to reflect the clinical scenario under which some patients with diabetes are treated. Based on this therapeutic approach, control of hyperglycaemia was observed in the MET group during the second IPGTT, whereas hyperglycaemia was maintained in the T2DM group. Animals in the MET group exhibited lower weight than those in the other two groups, in accordance with the clinical scenario<sup>103,104</sup>. Metformin-associated weight loss is attributable to modulation of the hypothalamic appetite-regulatory centres and alteration of the gut microbiome<sup>103</sup>, further confirming the effective administration of this medication at clinically relevant concentrations. The lack of difference between the body weight of CTRL and T2DM animals is probably due to the depletion of insulin secretion by STZ<sup>105-107</sup>, and the shifted muscle/fat ratio in the diabetic animals.

#### *V.1.1. Respiratory mechanical consequences*

Measurement of esophageal pressure using a miniature catheter-tip pressure transducer allows the separate assessment of lung and chest wall mechanics<sup>59,60</sup>. As diabetes and metformin therapy have minor effects on chest wall mechanics regardless of the PEEP, these well-validated assessments revealed the primary contribution of the abnormal pulmonary mechanics to the pathologic changes in the respiratory system following sustained hyperglycemia. These respiratory mechanical alterations confirmed previous findings of reduced airway patency and compromised lung tissue viscoelasticity at low PEEP, whereas increased PEEP can prevent deleterious changes in the lungs, thereby overcoming the detrimental lung mechanical consequences of diabetes<sup>48</sup>. The nTGV values in the T2DM group tended to be higher compared with the other protocol groups, which can be explained by small airway obstruction and gas trapping. However, the lack of significant differences in nTGV among the protocol groups indicates that the altered lung tissue mechanics in diabetes is of intrinsic origin, as opposed to resulting from a shift in static lung volumes. The primary involvement of intrinsic lung tissue remodeling in diabetes was further confirmed by the histological evidence of collagen overexpression in the pulmonary parenchyma. Pathological arrangement and cross-bridging of elastin-collagen fibers resulting from glycation determine the overall lung tissue viscoelasticity rather than their amounts<sup>108,109</sup>. T2DM may affect not only the amount but also the structural rearrangement of the elastic-collagen network subsequent to lung inflation, which may explain the apparent discrepancy between the PEEP-dependent mechanical and histological findings.

Regarding the alterations of the chest wall properties in diabetes, the significantly reduced  $\eta$  at low PEEP suggested the development of a shift toward elasticity at the expense of energy dissipation in the tissues forming the chest wall. The pathophysiological background of these findings is not completely clear. However, the trends of changes of G and H in diabetes indicate a somewhat stiffened fiber network of ECM associated with reduced internal friction within chest wall tissues. The trend of increased chest wall elastance is in line with previous results demonstrating increased passive stiffness of single skeletal muscle fibers in older adults with T2DM<sup>53</sup>. The reduced sensitivity of our measurements to detect alterations in skeletal muscle mechanics can be explained by the involvement of the cage bones and costal cartilage in our in vivo mechanical parameters. Due to the lack of an in vivo method to determine changes in the mechanical properties of these anatomical structures, the diabetes-related alterations of skeletal muscle mechanics were blunted.

#### *V.1.2. Effects of metformin therapy*

Another main finding of the present study was the ability of metformin to reduce the respiratory manifestations of T2DM. Metformin monotherapy lowers blood sugar by enhancing the insulin-mediated suppression of gluconeogenesis and increasing insulin-mediated glucose uptake in skeletal muscle<sup>110</sup>. Furthermore, the pleiotropic effects of metformin<sup>83</sup> may contribute to its ability to reduce inflammation<sup>111</sup>, oxidative stress<sup>112</sup>, endothelial remodeling, and proliferation of pulmonary vascular smooth muscle cells<sup>113</sup>. Phosphorylation of AMP-activated protein kinase influences the intracellular energy balance via lipid and glucose metabolism and inhibits transforming growth factor- $\beta$ -induced collagen production by fibroblasts<sup>114</sup>. All these mechanisms may have contributed to the reduced collagen accumulation in lung tissue and the normalized lung and chest wall mechanics in rats in the MET group. In accordance with previous results, T2DM increased intrapulmonary shunt and compromised lung oxygenation at low and high PEEP<sup>48</sup>. The elevated Qs/Qt and compromised PaO<sub>2</sub> at 0 cmH<sub>2</sub>O PEEP can be explained by the small airway obstruction and atelectasis, and these adverse phenomena were reversed to some extent by elevating PEEP to 3 cmH<sub>2</sub>O. Further elevating PEEP with the lack of hemodynamic response for the elevated intrathoracic pressure caused the additional compression of the pulmonary capillaries in the well-ventilated alveolar regions, thereby redirecting the perfusion to lung regions with somewhat poorer aeration. The gas-exchange outcomes in the MET group did not differ from those in the CTRL group. This finding demonstrates that the beneficial effects of metformin on respiratory mechanics were also manifested in the potential of this treatment to maintain physiological gas exchange.

## ***V.2. Modulation of VILI in models of treated and untreated T2DM***

This study has revealed the potential of T2DM to worsen respiratory functions and lung injury following a biotrauma of prolonged mechanical ventilation according to decline in parameters reflecting gas exchange. Lung histological and immunochemical parameters also showed that diabetes enhanced VILI and oxidative DNA damage. Metformin treatment prevented the detrimental pulmonary consequences of long-term mechanical ventilation in the presence of diabetes.

In this study, a well-established model was adapted to induce T2DM by administering a single low dose of STZ to induce diffuse degeneration of pancreatic cells to imitate beta cell insufficiency combined with high-fat diet<sup>86,115</sup>. The fasting glucose levels of the STZ-treated rats were consistently above the threshold of 7.0 mmol/L and their blood glucose levels were significantly higher compared to the control animals. Furthermore, the 120-min blood glucose values were above the threshold of 11.1 mmol/L in all STZ-treated animals, while none of the control animals had abnormal blood glucose values. Consequently, according to the diagnostic criteria<sup>116</sup>, rats in both STZ-treated groups (T2DM and MET groups) exhibited definitive blood glucose abnormalities characteristic to diabetes one week after the STZ treatment, before the initiation of metformin therapy. At the end of the pretreatment period, during the second tolerance test, the fasting and 120-min blood glucose values of the T2DM group exceeded both thresholds. The MET group showed a more controlled hyperglycaemia during the second test, while the blood glucose curves of the CTRL animals were identical during both tolerance tests (Figure 11).

### ***V.2.1. VILI in the presence of T2DM***

The translational animal model used in the present study aimed at mimicking the development of mild–moderate VILI in the absence of a pre-existing pulmonary disorder. Accordingly, we applied no intervention to induce surfactant deficiency or proinflammatory treatments before initiating the prolonged mechanical ventilation. The alveolar overdistension and enhanced lung parenchymal shear stress as key features of VILI were generated by a combined application of high VT and low PEEP to facilitate the development of barotrauma, volutrauma, and atelectrauma in the rats of all experimental groups<sup>102,117</sup>. Irrespective of the presence of T2DM, these mechanical stresses were manifested in deterioration in gas exchange (Figure 12) and in lung injury and oxidative DNA damage (Figures 14, 15). Interestingly, although a decline in the mechanical properties of the respiratory system due to the injurious ventilation was

indicated by significant elevations in PIP in the T2DM group, the changes in the forced oscillatory parameters did not reach significance during the study period (Figure 13). This result can be explained by the application of excessively high VTs during the injurious ventilation (more than three times the normal) that assured maximal alveolar recruitment during the study period<sup>118</sup>. Moreover, the involvement of a significantly unaffected chest wall component in G and H may have blunted the sensitivity of these mechanical outcomes to detect mild–moderate lung injury<sup>59</sup>. Conversely, markedly greater LIS and overexpression of 8-OHGD-positive cells in the lung tissue were observed in CTRL animals than those obtained in previous experiments in naïve rats without injurious ventilation ( $0.15 \pm 0.12$  vs.  $0.49 \pm 0.18$  and  $3.0 \pm 1.0$  vs.  $7.0 \pm 2.9$ ,  $p < 0.05$  for both)<sup>48</sup>. These findings confirm the development of the structural and functional pathologies characteristic of VILI even in the control animals without metabolic disorder.

The most remarkable finding of the present study is the exaggeration of VILI in rats with untreated T2DM. The more severe detrimental consequences of untreated T2DM were evidenced by the greater magnitude of deteriorations in the gas exchange ability of the lungs and parameters reflecting  $Q_s/Q_t$  (Figure 12). As the respiratory mechanical parameters did not exhibit an excessive change in rats with diabetes, atelectatic lung volume loss was not likely to play a major role in the excessively compromised gas exchange (Figure 13). Alternatively, the exaggerated impairment of gas exchange in the diabetic animals can be attributed to the intrinsic lung tissue remodelling and inflammation with an impaired alveolar–capillary barrier, all leading to a reduced diffusion of gas molecules through the alveolar membrane. The involvement of this mechanism is confirmed by the histological findings evidencing alveolar septal congestion and haemorrhage associated with intra-alveolar deposition of fibrin and infiltrates (Figure 15). In accordance with our findings, previous studies have also demonstrated direct tissue damage in experimental models of VILI due to inflammation and oxidative damage of cellular components. These include oxidation of tissue lipid and protein components<sup>119,120</sup>, increased levels of IL-1 $\beta$ , IL-6, IL-8, and TNF- $\alpha$ <sup>121</sup>. These molecular processes enhance the proinflammatory effects of prolonged hyperglycaemia<sup>42,122</sup>, resulting in more severe lung injury.

### *V.2.2. Effects of metformin therapy*

A further noteworthy finding of this study is the ability of metformin to prevent the worsening of VILI subsequent to T2DM. The results of the 2nd IPGTT performed after metformin

treatments demonstrated the effectiveness of this therapy in leading to controlled hyperglycaemia in the MET group through the following well-established mechanisms of action: inhibiting hepatic gluconeogenesis and reducing hepatic glucose output; increasing glucose uptake and utilization in peripheral tissues (muscle and fat); and improving energy metabolism in the muscle, fat, and liver through the activation of AMP-activated protein kinase<sup>123</sup>. It has been described that the AMP-activated protein kinase down-regulated inflammatory pathways such as the NF- $\kappa$ B pathway<sup>124</sup>, which might contribute to the beneficial respiratory effects of metformin. Consistent with previous results, metformin therapy had no significant effects on the baseline lung functional or structural parameters<sup>125</sup>. However, the effects of this first-line antidiabetic therapy on the lungs were clearly manifested in the potential to prevent the T2DM-induced excessive worsening in gas exchange (Figure 12), the aggravation of lung injury (Figure 13), and the oxidative DNA damage (Figure 14). These findings suggest the ability of metformin therapy to not only reduce hyperglycaemia and impaired glucose tolerance but also abolish the adverse pulmonary consequences of T2DM. Our results correspond to previous experimental and clinical findings demonstrating that adequate diabetes therapy prevents the development of lung injury as a complication of mechanical ventilation<sup>83,126</sup>, although excessive hyperglycaemia results in elevated expression of pro-inflammatory cytokines leading to severe lung injury<sup>127,128</sup>.

### ***V.3. Limitations of the studies***

#### ***V.3.1. Effect of T2DM on the PEEP-dependent respiratory mechanics***

Due to cyclic hormonal changes in female rats, previous studies described that the STZ and HFD receiving T2DM models are more stable in male rats. Thus, our study design does not allow the assessment of possible sex-related differences. Our protocol was designed to initiate metformin treatment after 6 weeks of high-fat diet feeding for weeks following STZ treatment, i.e., after the development of T2DM as proven by the first IPGTT. Although we aimed to use a well-established T2DM model in our study, the STZ treatment has several adverse effects, which may influence the result obtained. A relevant limitation to the present study is that the proinflammatory and fibrogenic influence can be a part of both long-term hyperglycaemia and STZ treatment<sup>129</sup>. Although this protocol design mimics the clinical scenario under which metformin is administered after the development of T2DM, it is not straightforward to assess whether metformin corrected T2DM-induced adverse alterations in the lungs or prevented the progression of metabolic disorder. This can be a subject of further investigation in which the

changes in the lung mechanical and gas-exchange parameters are followed for sufficient time during the treatment period.

### *V.3.2. Modulation of VILI in models of treated and untreated T2DM*

Well-established models for treated and untreated T2DM were used in this study that reflect the pathogenesis of the human metabolic disease, including the chronic hyperglycaemia, impaired glucose tolerance, and all consequential adverse pulmonary and systemic outcomes<sup>130</sup>. However, the antidiabetic medication was applied through drinking water. Hence, rats in the MET group represent a patient population with high medication adherence, which represents only a fragment of patient population with treated diabetes<sup>131</sup>. A further technical aspect of this research protocol is the application of a relatively short injurious ventilation period (4 h). This time interval is equivalent to a far longer ventilation period in human subjects due to the significantly greater ventilation frequency in rats, and thus, such regimen has been used in numerous earlier studies to induce VILI in animals with healthy lungs<sup>102,132</sup>. However, a more prolonged ventilation period may further augment the severity of VILI in the presence of T2DM, particularly if diabetes is associated with a chronic pulmonary disease, such as Chronic Obstructive Pulmonary Disease<sup>133</sup>; these aspects may be subjects of further investigations. Our study evidenced an enhanced DNA damage after injurious ventilation in the presence of diabetes. However, evaluation of further biomarkers related to oxidative stress would be needed to confirm the role of this mechanism in pulmonary tissue damage and the exaggerated lung injury in the concordant presence of VILI and untreated T2DM.

## **VI. SUMMARY AND CONCLUSIONS**

The investigations detailed in the present thesis reveal novel aspects of the respiratory consequences of T2DM, with particular focus on the PEEP-dependence of lung and chest wall mechanics and on the potential of T2DM to modulate lung injury following a prolonged mechanical ventilation.

As a summary of the results on how treated or untreated T2DM affect the PEEP-dependent respiratory mechanics, our findings have led to the following conclusions:

- I. Separate measurements of the lung and chest wall mechanical properties demonstrated the primary involvement of the pulmonary system in the global deterioration of total respiratory system mechanics following the development of diabetes.

- II. Sustained hyperglycaemia compromised airway patency, increased lung parenchymal stiffness and energy loss along with increased atelectasis development at low PEEP.
- III. These adverse pulmonary changes were associated with the overexpression of extracellular collagen fibres in lung tissue.
- IV. Gas exchange was compromised due to the increased risk of atelectasis development at low PEEP levels and due to the remodelling of the alveolocapillary barrier and the augmented compressibility of intraalveolar capillaries at high PEEP.
- V. The mild mechanical consequence of chronic hyperglycaemia on the viscoelastic properties of chest wall tissues was only manifested as a decrease in tissue damping at a low PEEP level, demonstrating a mechanical shift toward the dominance of elastic stresses over internal frictional forces.

The results of a further study assessing how models of treated and untreated T2DM modulate lung injury after a prolonged mechanical ventilation revealed the following main findings:

- VI. Prolonged mechanical ventilation of diabetic lungs aggravates the functional and structural manifestations of mild–moderate VILI.
- VII. Exaggerated lung injury in a model of T2DM results in more severe remodelling of the alveolar–capillary barrier, and this is the primary cause of the declined gas exchange following prolonged injurious mechanical ventilation.
- VIII. Although major deterioration in gas exchange and respiratory mechanics has not been observed after injurious ventilation, the enhanced inflammation and the tissue damage in a model of T2DM may be warning signs of a more severe long-term consequences in the respiratory system.

Finally, the effects of a standard diabetes therapy with metformin were assessed in the respiratory consequences of T2DM in both studies included in the present thesis, with results demonstrating:

- IX. Early and adequate metformin therapy effectively treats the adverse respiratory consequences of diabetes, in addition to its well-established beneficial systemic effects.
- X. Although metformin therapy has no direct effect on lung function or gas exchange, controlled hyperglycaemia or euglycemia lowers the risk of developing ALI and, in severe cases, the development of ARDS subsequent to long-term mechanical ventilation.
- XI. Considering these findings together further emphasize the importance of the early diagnosis and therapy in diabetes.

In conclusion, these findings have particular relevance for both improving our understanding of breathing difficulties in diabetes and optimizing anaesthesia management and intensive care requiring mechanical ventilation in this patient population, which is susceptible to respiratory complications.

## VII. ACKNOWLEDGEMENTS

First of all, I would like to express my thanks and gratitude to my supervisors. More than six years ago I joined the cardiopulmonary research group led by Professor Ferenc Peták and Professor Barna Babik. They helped me with their immense knowledge and dedication during my university years and then during my PhD studies. Without their help and guidance, I could not be able to complete this journey. They have greatly influenced me.

I am grateful to Roberta Südy. From the very beginning, she has been the most supporting person and a very close friend to this day. Everything I know about how to perform experiments, she taught me. I would like to thank Gergely Fodor for his help in carrying out the experiments and data analysis. He is an amazing lab mate and a good friend. I am grateful to Professor Walid Habre for the opportunity joining his research lab. His work has had the biggest influence on my career.

I would like to thank József Tolnai for helping me in data analysis and to Orsolya Ivánkovitsné Kiss for her enormous technical help in all the experiments. I would like to thank to Ádám Balogh for his advice during my research career and to Viktória Varga for the great help with the histological analyses. I am thankful to Bence Ballók and Richard Kulcsár for their help carrying out the experiments. I thank to Noémi Schwartz for being the best friend since the beginning of the medical school. And lastly, my biggest appreciation to my family for their support.

## VIII. REFERENCES

1. Stumvoll M, Goldstein BJ, van Haeften TW: Type 2 diabetes: principles of pathogenesis and therapy. *Lancet* 2005; 365: 1333-46
2. Sun H, Saeedi P, Karuranga S, Pinkepank M, Ogurtsova K, Duncan BB, Stein C, Basit A, Chan JCN, Mbanya JC, Pavkov ME, Ramachandaran A, Wild SH, James S, Herman WH, Zhang P, Bommer C, Kuo S, Boyko EJ, Magliano DJ: IDF Diabetes Atlas: Global, regional and country-level diabetes prevalence estimates for 2021 and projections for 2045. *Diabetes Res Clin Pract* 2022; 183: 109119
3. Gallagher C, Moschonis G, Lambert KA, Karaglani E, Mavrogianni C, Gavrili S, Manios Y, Erbas B: Sugar-sweetened beverage consumption is associated with visceral fat in children. *Br J Nutr* 2021; 125: 819-827
4. Mayer-Davis EJ, Lawrence JM, Dabelea D, Divers J, Isom S, Dolan L, Imperatore G, Linder B, Marcovina S, Pettitt DJ, Pihoker C, Saydah S, Wagenknecht L, Study SfdiY: Incidence Trends of Type 1 and Type 2 Diabetes among Youths, 2002-2012. *N Engl J Med* 2017; 376: 1419-1429
5. Zand A, Ibrahim K, Patham B: Prediabetes: Why Should We Care? *Methodist Debakey Cardiovasc J* 2018; 14: 289-297
6. Tabak AG, Herder C, Rathmann W, Brunner EJ, Kivimaki M: Prediabetes: a high-risk state for diabetes development. *Lancet* 2012; 379: 2279-90
7. Richter B, Hemmingsen B, Metzendorf MI, Takwoingi Y: Development of type 2 diabetes mellitus in people with intermediate hyperglycaemia. *Cochrane Database Syst Rev* 2018; 10: CD012661
8. Huang Y, Cai X, Mai W, Li M, Hu Y: Association between prediabetes and risk of cardiovascular disease and all cause mortality: systematic review and meta-analysis. *BMJ* 2016; 355: i5953
9. Carris NW, Magness RR, Labovitz AJ: Prevention of Diabetes Mellitus in Patients With Prediabetes. *Am J Cardiol* 2019; 123: 507-512
10. Diabetes Prevention Program Research G, Knowler WC, Fowler SE, Hamman RF, Christophi CA, Hoffman HJ, Brenneman AT, Brown-Friday JO, Goldberg R, Venditti E, Nathan DM: 10-year follow-up of diabetes incidence and weight loss in the Diabetes Prevention Program Outcomes Study. *Lancet* 2009; 374: 1677-86
11. Kahn CR: Banting Lecture. Insulin action, diabetogenes, and the cause of type II diabetes. *Diabetes* 1994; 43: 1066-84
12. Robertson RP: Antagonist: diabetes and insulin resistance--philosophy, science, and the multiplier hypothesis. *J Lab Clin Med* 1995; 125: 560-4; discussion 565
13. Lv C, Sun Y, Zhang ZY, Aboelela Z, Qiu X, Meng ZX: beta-cell dynamics in type 2 diabetes and in dietary and exercise interventions. *J Mol Cell Biol* 2022; 14
14. Hudish LI, Reusch JE, Sussel L: beta Cell dysfunction during progression of metabolic syndrome to type 2 diabetes. *J Clin Invest* 2019; 129: 4001-4008
15. Beck-Nielsen H, Groop LC: Metabolic and genetic characterization of prediabetic states. Sequence of events leading to non-insulin-dependent diabetes mellitus. *J Clin Invest* 1994; 94: 1714-21
16. Grarup N, Sandholt CH, Hansen T, Pedersen O: Genetic susceptibility to type 2 diabetes and obesity: from genome-wide association studies to rare variants and beyond. *Diabetologia* 2014; 57: 1528-41
17. Rosengren AH, Braun M, Mahdi T, Andersson SA, Travers ME, Shigeto M, Zhang E, Almgren P, Ladenvall C, Axelsson AS, Edlund A, Pedersen MG, Jonsson A, Ramracheya R, Tang Y, Walker JN, Barrett A, Johnson PR, Lyssenko V, McCarthy MI, Groop L, Salehi A,

- Gloyn AL, Renstrom E, Rorsman P, Eliasson L: Reduced insulin exocytosis in human pancreatic beta-cells with gene variants linked to type 2 diabetes. *Diabetes* 2012; 61: 1726-33
18. Dupuis J, Langenberg C, Prokopenko I, Saxena R, Soranzo N, Jackson AU, Wheeler E, Glazer NL, Bouatia-Naji N, Gloyn AL, Lindgren CM, Magi R, Morris AP, Randall J, Johnson T, Elliott P, Rybin D, Thorleifsson G, Steinthorsdottir V, Henneman P, Grallert H, Dehghan A, Hottenga JJ, Franklin CS, Navarro P, Song K, Goel A, Perry JR, Egan JM, Lajunen T, Grarup N, Sparso T, Doney A, Voight BF, Stringham HM, Li M, Kanoni S, Shrader P, Cavalcanti-Proenca C, Kumari M, Qi L, Timpson NJ, Gieger C, Zabena C, Rocheleau G, Ingelsson E, An P, O'Connell J, Luan J, Elliott A, McCarroll SA, Payne F, Roccasecca RM, Pattou F, Sethupathy P, Ardlie K, Ariyurek Y, Balkau B, Barter P, Beilby JP, Ben-Shlomo Y, Benediktsson R, Bennett AJ, Bergmann S, Bochud M, Boerwinkle E, Bonnefond A, Bonnycastle LL, Borch-Johnsen K, Bottcher Y, Brunner E, Bumpstead SJ, Charpentier G, Chen YD, Chines P, Clarke R, Coin LJ, Cooper MN, Cornelis M, Crawford G, Crisponi L, Day IN, de Geus EJ, Delplanque J, Dina C, Erdos MR, Fedson AC, Fischer-Rosinsky A, Forouhi NG, Fox CS, Frants R, Franzosi MG, Galan P, Goodarzi MO, Graessler J, Groves CJ, Grundy S, Gwilliam R, Gyllensten U, Hadjadj S, et al.: New genetic loci implicated in fasting glucose homeostasis and their impact on type 2 diabetes risk. *Nat Genet* 2010; 42: 105-16
19. Manning AK, Hivert MF, Scott RA, Grimsby JL, Bouatia-Naji N, Chen H, Rybin D, Liu CT, Bielak LF, Prokopenko I, Amin N, Barnes D, Cadby G, Hottenga JJ, Ingelsson E, Jackson AU, Johnson T, Kanoni S, Ladenvall C, Lagou V, Lahti J, Lecoeur C, Liu Y, Martinez-Larrad MT, Montasser ME, Navarro P, Perry JR, Rasmussen-Torvik LJ, Salo P, Sattar N, Shungin D, Strawbridge RJ, Tanaka T, van Duijn CM, An P, de Andrade M, Andrews JS, Aspelund T, Atalay M, Aulchenko Y, Balkau B, Bandinelli S, Beckmann JS, Beilby JP, Bellis C, Bergman RN, Blangero J, Boban M, Boehnke M, Boerwinkle E, Bonnycastle LL, Boomsma DI, Borecki IB, Bottcher Y, Bouchard C, Brunner E, Budimir D, Campbell H, Carlson O, Chines PS, Clarke R, Collins FS, Corbaton-Anchuelo A, Couper D, de Faire U, Dedoussis GV, Deloukas P, Dimitriou M, Egan JM, Eiriksdottir G, Erdos MR, Eriksson JG, Eury E, Ferrucci L, Ford I, Forouhi NG, Fox CS, Franzosi MG, Franks PW, Frayling TM, Froguel P, Galan P, de Geus E, Gigante B, Glazer NL, Goel A, Groop L, Gudnason V, Hallmans G, Hamsten A, Hansson O, Harris TB, Hayward C, Heath S, Hercberg S, Hicks AA, Hingorani A, Hofman A, Hui J, Hung J, et al.: A genome-wide approach accounting for body mass index identifies genetic variants influencing fasting glycemic traits and insulin resistance. *Nat Genet* 2012; 44: 659-69
20. Morris AP, Voight BF, Teslovich TM, Ferreira T, Segre AV, Steinthorsdottir V, Strawbridge RJ, Khan H, Grallert H, Mahajan A, Prokopenko I, Kang HM, Dina C, Esko T, Fraser RM, Kanoni S, Kumar A, Lagou V, Langenberg C, Luan J, Lindgren CM, Muller-Nurasyid M, Pechlivanis S, Rayner NW, Scott LJ, Wiltshire S, Yengo L, Kinnunen L, Rossin EJ, Raychaudhuri S, Johnson AD, Dimas AS, Loos RJ, Vedantam S, Chen H, Florez JC, Fox C, Liu CT, Rybin D, Couper DJ, Kao WH, Li M, Cornelis MC, Kraft P, Sun Q, van Dam RM, Stringham HM, Chines PS, Fischer K, Fontanillas P, Holmen OL, Hunt SE, Jackson AU, Kong A, Lawrence R, Meyer J, Perry JR, Platou CG, Potter S, Rehnberg E, Robertson N, Sivapalaratnam S, Stancakova A, Stirrups K, Thorleifsson G, Tikkanen E, Wood AR, Almgren P, Atalay M, Benediktsson R, Bonnycastle LL, Burt N, Carey J, Charpentier G, Crenshaw AT, Doney AS, Dorkhan M, Edkins S, Emilsson V, Eury E, Forsen T, Gertow K, Gigante B, Grant GB, Groves CJ, Guiducci C, Herder C, Hreidarsson AB, Hui J, James A, Jonsson A, Rathmann W, Klopp N, Kravic J, Krjutskov K, Langford C, Leander K, Lindholm E, Lobbens S, Mannisto S, et al.: Large-scale association analysis provides insights into the genetic architecture and pathophysiology of type 2 diabetes. *Nat Genet* 2012; 44: 981-90

21. Evans-Molina C, Garmey JC, Ketchum R, Brayman KL, Deng S, Mirmira RG: Glucose regulation of insulin gene transcription and pre-mRNA processing in human islets. *Diabetes* 2007; 56: 827-35
22. Guest PC, Bailyes EM, Rutherford NG, Hutton JC: Insulin secretory granule biogenesis. Co-ordinate regulation of the biosynthesis of the majority of constituent proteins. *Biochem J* 1991; 274 ( Pt 1): 73-8
23. Vasiljevic J, Torkko JM, Knoch KP, Solimena M: The making of insulin in health and disease. *Diabetologia* 2020; 63: 1981-1989
24. Butler AE, Janson J, Bonner-Weir S, Ritzel R, Rizza RA, Butler PC: Beta-cell deficit and increased beta-cell apoptosis in humans with type 2 diabetes. *Diabetes* 2003; 52: 102-10
25. Hanley SC, Austin E, Assouline-Thomas B, Kapeluto J, Blaichman J, Moosavi M, Petropavlovskaja M, Rosenberg L: beta-Cell mass dynamics and islet cell plasticity in human type 2 diabetes. *Endocrinology* 2010; 151: 1462-72
26. Rahier J, Guiot Y, Goebbels RM, Sempoux C, Henquin JC: Pancreatic beta-cell mass in European subjects with type 2 diabetes. *Diabetes Obes Metab* 2008; 10 Suppl 4: 32-42
27. Eizirik DL, Pasquali L, Cnop M: Pancreatic beta-cells in type 1 and type 2 diabetes mellitus: different pathways to failure. *Nat Rev Endocrinol* 2020; 16: 349-362
28. Cnop M, Vidal J, Hull RL, Utzschneider KM, Carr DB, Schraw T, Scherer PE, Boyko EJ, Fujimoto WY, Kahn SE: Progressive loss of beta-cell function leads to worsening glucose tolerance in first-degree relatives of subjects with type 2 diabetes. *Diabetes Care* 2007; 30: 677-82
29. Green DR, Oguin TH, Martinez J: The clearance of dying cells: table for two. *Cell Death Differ* 2016; 23: 915-26
30. Sullivan PW, Morrato EH, Ghushchyan V, Wyatt HR, Hill JO: Obesity, inactivity, and the prevalence of diabetes and diabetes-related cardiovascular comorbidities in the U.S., 2000-2002. *Diabetes Care* 2005; 28: 1599-603
31. Weinstein AR, Sesso HD, Lee IM, Cook NR, Manson JE, Buring JE, Gaziano JM: Relationship of physical activity vs body mass index with type 2 diabetes in women. *JAMA* 2004; 292: 1188-94
32. Venkatasamy VV, Pericherla S, Manthuruthil S, Mishra S, Hanno R: Effect of Physical activity on Insulin Resistance, Inflammation and Oxidative Stress in Diabetes Mellitus. *J Clin Diagn Res* 2013; 7: 1764-6
33. Strasser B: Physical activity in obesity and metabolic syndrome. *Ann N Y Acad Sci* 2013; 1281: 141-59
34. Ouchi N, Parker JL, Lugus JJ, Walsh K: Adipokines in inflammation and metabolic disease. *Nat Rev Immunol* 2011; 11: 85-97
35. Danforth E, Jr.: Failure of adipocyte differentiation causes type II diabetes mellitus? *Nat Genet* 2000; 26: 13
36. Kolb H, Martin S: Environmental/lifestyle factors in the pathogenesis and prevention of type 2 diabetes. *BMC Med* 2017; 15: 131
37. Al-Mansoori L, Al-Jaber H, Prince MS, Elrayess MA: Role of Inflammatory Cytokines, Growth Factors and Adipokines in Adipogenesis and Insulin Resistance. *Inflammation* 2022; 45: 31-44
38. Saitoh S, Van Wijk K, Nakajima O: Crosstalk between Metabolic Disorders and Immune Cells. *Int J Mol Sci* 2021; 22
39. Babik B, Petak F, Agocs S, Blaskovics I, Alacs E, Bodo K, Sudy R: [Diabetes mellitus: endothelial dysfunction and changes in hemostasis]. *Orv Hetil* 2018; 159: 1335-1345
40. Mostafizar M, Cortes-Perez C, Snow W, Djordjevic J, Adlimoghaddam A, Albensi BC: Challenges with Methods for Detecting and Studying the Transcription Factor Nuclear Factor Kappa B (NF-kappaB) in the Central Nervous System. *Cells* 2021; 10

41. Brownlee M: The pathobiology of diabetic complications: a unifying mechanism. *Diabetes* 2005; 54: 1615-25
42. Brownlee M: Biochemistry and molecular cell biology of diabetic complications. *Nature* 2001; 414: 813-20
43. Rajasurya V, Gunasekaran K, Surani S: Interstitial lung disease and diabetes. *World J Diabetes* 2020; 11: 351-357
44. Zheng H, Wu J, Jin Z, Yan LJ: Potential Biochemical Mechanisms of Lung Injury in Diabetes. *Aging Dis* 2017; 8: 7-16
45. Klein OL, Krishnan JA, Glick S, Smith LJ: Systematic review of the association between lung function and Type 2 diabetes mellitus. *Diabet Med* 2010; 27: 977-87
46. Lecube A, Simo R, Pallayova M, Punjabi NM, Lopez-Cano C, Turino C, Hernandez C, Barbe F: Pulmonary Function and Sleep Breathing: Two New Targets for Type 2 Diabetes Care. *Endocr Rev* 2017; 38: 550-573
47. Sahebjami H, Denholm D: Effects of streptozotocin-induced diabetes on lung mechanics and biochemistry in rats. *J Appl Physiol* (1985) 1988; 64: 147-53
48. Sudy R, Schranc A, Fodor GH, Tolnai J, Babik B, Petak F: Lung volume dependence of respiratory function in rodent models of diabetes mellitus. *Respir Res* 2020; 21: 82
49. Sudy R, Petak F, Kiss L, Balogh AL, Fodor GH, Korsos A, Schranc A, Babik B: Obesity and diabetes: similar respiratory mechanical but different gas exchange defects. *Am J Physiol Lung Cell Mol Physiol* 2021; 320: L368-L376
50. Pitocco D, Fuso L, Conte EG, Zaccardi F, Condoluci C, Scavone G, Incalzi RA, Ghirlanda G: The diabetic lung--a new target organ? *Rev Diabet Stud* 2012; 9: 23-35
51. American Diabetes A: 2. Classification and Diagnosis of Diabetes: Standards of Medical Care in Diabetes-2020. *Diabetes Care* 2020; 43: S14-S31
52. Ahmad K, Choi I, Lee YH: Implications of Skeletal Muscle Extracellular Matrix Remodeling in Metabolic Disorders: Diabetes Perspective. *Int J Mol Sci* 2020; 21
53. Lee EJ, Jang HC, Koo KH, Kim HY, Lim JY: Mechanical Properties of Single Muscle Fibers: Understanding Poor Muscle Quality in Older Adults with Diabetes. *Ann Geriatr Med Res* 2020; 24: 267-273
54. Ahmad K, Shaikh S, Lee EJ, Lee YH, Choi I: Consequences of Dicarbonyl Stress on Skeletal Muscle Proteins in Type 2 Diabetes. *Curr Protein Pept Sci* 2020; 21: 878-889
55. Reyaz A, Alam S, Chandra K, Kohli S, Agarwal S: Methylglyoxal and soluble RAGE in type 2 diabetes mellitus: Association with oxidative stress. *J Diabetes Metab Disord* 2020; 19: 515-521
56. Davis HM, Essex AL, Valdez S, Deosthale PJ, Aref MW, Allen MR, Bonetto A, Plotkin LI: Short-term pharmacologic RAGE inhibition differentially affects bone and skeletal muscle in middle-aged mice. *Bone* 2019; 124: 89-102
57. Chiu CY, Yang RS, Sheu ML, Chan DC, Yang TH, Tsai KS, Chiang CK, Liu SH: Advanced glycation end-products induce skeletal muscle atrophy and dysfunction in diabetic mice via a RAGE-mediated, AMPK-down-regulated, Akt pathway. *J Pathol* 2016; 238: 470-82
58. Guerin C, Bayat S, Noury N, Cour M, Argaud L, Louis B, Terzi N: Regional lung viscoelastic properties in supine and prone position in a porcine model of acute respiratory distress syndrome. *J Appl Physiol* (1985) 2021; 131: 15-25
59. Sudy R, Fodor GH, Dos Santos Rocha A, Schranc A, Tolnai J, Habre W, Petak F: Different contributions from lungs and chest wall to respiratory mechanics in mice, rats, and rabbits. *J Appl Physiol* (1985) 2019; 127: 198-204
60. Petak F, Hall GL, Sly PD: Repeated measurements of airway and parenchymal mechanics in rats by using low-frequency oscillations. *J Appl Physiol* (1985) 1998; 84: 1680-6
61. LaMoia TE, Shulman GI: Cellular and Molecular Mechanisms of Metformin Action. *Endocr Rev* 2021; 42: 77-96

62. Johnson AB, Webster JM, Sum CF, Heseltine L, Argyraki M, Cooper BG, Taylor R: The impact of metformin therapy on hepatic glucose production and skeletal muscle glycogen synthase activity in overweight type II diabetic patients. *Metabolism* 1993; 42: 1217-22
63. El-Mir MY, Nogueira V, Fontaine E, Averet N, Rigoulet M, Leverve X: Dimethylbiguanide inhibits cell respiration via an indirect effect targeted on the respiratory chain complex I. *J Biol Chem* 2000; 275: 223-8
64. Takashima M, Ogawa W, Hayashi K, Inoue H, Kinoshita S, Okamoto Y, Sakaue H, Wataoka Y, Emi A, Senga Y, Matsuki Y, Watanabe E, Hiramatsu R, Kasuga M: Role of KLF15 in regulation of hepatic gluconeogenesis and metformin action. *Diabetes* 2010; 59: 1608-15
65. Fullerton MD, Galic S, Marcinko K, Sikkema S, Pulinilkunnil T, Chen ZP, O'Neill HM, Ford RJ, Palanivel R, O'Brien M, Hardie DG, Macaulay SL, Schertzer JD, Dyck JR, van Denderen BJ, Kemp BE, Steinberg GR: Single phosphorylation sites in Acc1 and Acc2 regulate lipid homeostasis and the insulin-sensitizing effects of metformin. *Nat Med* 2013; 19: 1649-54
66. Nosadini R, Avogaro A, Trevisan R, Valerio A, Tessari P, Duner E, Tiengo A, Velussi M, Del Prato S, De Kreutzenberg S, et al.: Effect of metformin on insulin-stimulated glucose turnover and insulin binding to receptors in type II diabetes. *Diabetes Care* 1987; 10: 62-7
67. Forslund K, Hildebrand F, Nielsen T, Falony G, Le Chatelier E, Sunagawa S, Prifti E, Vieira-Silva S, Gudmundsdottir V, Pedersen HK, Arumugam M, Kristiansen K, Voigt AY, Vestergaard H, Herczeg R, Costea PI, Kultima JR, Li J, Jorgensen T, Levenez F, Dore J, Meta HITc, Nielsen HB, Brunak S, Raes J, Hansen T, Wang J, Ehrlich SD, Bork P, Pedersen O: Disentangling type 2 diabetes and metformin treatment signatures in the human gut microbiota. *Nature* 2015; 528: 262-266
68. Coll AP, Chen M, Taskar P, Rimmington D, Patel S, Tadross JA, Cimino I, Yang M, Welsh P, Virtue S, Goldspink DA, Miedzybrodzka EL, Konopka AR, Esponda RR, Huang JT, Tung YCL, Rodriguez-Cuenca S, Tomaz RA, Harding HP, Melvin A, Yeo GSH, Preiss D, Vidal-Puig A, Vallier L, Nair KS, Wareham NJ, Ron D, Gribble FM, Reimann F, Sattar N, Savage DB, Allan BB, O'Rahilly S: GDF15 mediates the effects of metformin on body weight and energy balance. *Nature* 2020; 578: 444-448
69. Diabetes Prevention Program Research G: Long-term effects of lifestyle intervention or metformin on diabetes development and microvascular complications over 15-year follow-up: the Diabetes Prevention Program Outcomes Study. *Lancet Diabetes Endocrinol* 2015; 3: 866-75
70. Rojas LB, Gomes MB: Metformin: an old but still the best treatment for type 2 diabetes. *Diabetol Metab Syndr* 2013; 5: 6
71. Slutsky AS: Lung injury caused by mechanical ventilation. *Chest* 1999; 116: 9S-15S
72. Slutsky AS, Ranieri VM: Ventilator-induced lung injury. *N Engl J Med* 2013; 369: 2126-36
73. Talmor D, Sarge T, O'Donnell CR, Ritz R, Malhotra A, Lisbon A, Loring SH: Esophageal and transpulmonary pressures in acute respiratory failure. *Crit Care Med* 2006; 34: 1389-94
74. Faridy EE, Permutt S, Riley RL: Effect of ventilation on surface forces in excised dogs' lungs. *J Appl Physiol* 1966; 21: 1453-62
75. Dreyfuss D, Soler P, Basset G, Saumon G: High inflation pressure pulmonary edema. Respective effects of high airway pressure, high tidal volume, and positive end-expiratory pressure. *Am Rev Respir Dis* 1988; 137: 1159-64
76. Webb HH, Tierney DF: Experimental pulmonary edema due to intermittent positive pressure ventilation with high inflation pressures. Protection by positive end-expiratory pressure. *Am Rev Respir Dis* 1974; 110: 556-65
77. Albert RK: The role of ventilation-induced surfactant dysfunction and atelectasis in causing acute respiratory distress syndrome. *Am J Respir Crit Care Med* 2012; 185: 702-8

78. Dolinay T, Kim YS, Howrylak J, Hunninghake GM, An CH, Fredenburgh L, Massaro AF, Rogers A, Gazourian L, Nakahira K, Haspel JA, Landazury R, Eppanapally S, Christie JD, Meyer NJ, Ware LB, Christiani DC, Ryter SW, Baron RM, Choi AM: Inflammasome-regulated cytokines are critical mediators of acute lung injury. *Am J Respir Crit Care Med* 2012; 185: 1225-34
79. Curley GF, Laffey JG, Zhang H, Slutsky AS: Biotrauma and Ventilator-Induced Lung Injury: Clinical Implications. *Chest* 2016; 150: 1109-1117
80. Beitler JR, Malhotra A, Thompson BT: Ventilator-induced Lung Injury. *Clin Chest Med* 2016; 37: 633-646
81. Haberthur C, Seeberger MD: Acute respiratory distress syndrome and mechanical ventilation: ups and downs of an ongoing relationship trap. *J Thorac Dis* 2016; 8: E1608-E1609
82. Yu S, Christiani DC, Thompson BT, Bajwa EK, Gong MN: Role of diabetes in the development of acute respiratory distress syndrome. *Crit Care Med* 2013; 41: 2720-32
83. Tsaknis G, Siempos II, Kopterides P, Maniatis NA, Magkou C, Kardara M, Panoutsou S, Kotanidou A, Roussos C, Armaganidis A: Metformin attenuates ventilator-induced lung injury. *Crit Care* 2012; 16: R134
84. Percie du Sert N, Hurst V, Ahluwalia A, Alam S, Avey MT, Baker M, Browne WJ, Clark A, Cuthill IC, Dirnagl U, Emerson M, Garner P, Holgate ST, Howells DW, Karp NA, Lazic SE, Lidster K, MacCallum CJ, Macleod M, Pearl EJ, Petersen OH, Rawle F, Reynolds P, Rooney K, Sena ES, Silberberg SD, Steckler T, Wurbel H: The ARRIVE guidelines 2.0: Updated guidelines for reporting animal research. *PLoS Biol* 2020; 18: e3000410
85. Zhang M, Lv XY, Li J, Xu ZG, Chen L: The characterization of high-fat diet and multiple low-dose streptozotocin induced type 2 diabetes rat model. *Exp Diabetes Res* 2008; 2008: 704045
86. Skovso S: Modeling type 2 diabetes in rats using high fat diet and streptozotocin. *J Diabetes Investig* 2014; 5: 349-58
87. Garg G, Singh S, Singh AK, Rizvi SI: Metformin Alleviates Altered Erythrocyte Redox Status During Aging in Rats. *Rejuvenation Res* 2017; 20: 15-24
88. Liu CH, Hua N, Fu X, Pan YL, Li B, Li XD: Metformin regulates atrial SK2 and SK3 expression through inhibiting the PKC/ERK signaling pathway in type 2 diabetic rats. *BMC Cardiovasc Disord* 2018; 18: 236
89. Antunes LC, Elkfury JL, Jornada MN, Foletto KC, Bertoluci MC: Validation of HOMA-IR in a model of insulin-resistance induced by a high-fat diet in Wistar rats. *Arch Endocrinol Metab* 2016; 60: 138-42
90. Pilon S, Holloway AC, Thomson EM: Metabolic, stress, and inflammatory biomarker responses to glucose administration in Fischer-344 rats: intraperitoneal vs. oral delivery. *J Pharmacol Toxicol Methods* 2018; 90: 1-6
91. Wang X, Zhao X, Zhou R, Gu Y, Zhu X, Tang Z, Yuan X, Chen W, Zhang R, Qian C, Cui S: Delay in glucose peak time during the oral glucose tolerance test as an indicator of insulin resistance and insulin secretion in type 2 diabetes patients. *J Diabetes Investig* 2018; 9: 1288-1295
92. Wagner PD: The physiological basis of pulmonary gas exchange: implications for clinical interpretation of arterial blood gases. *Eur Respir J* 2015; 45: 227-43
93. Petak F, Hantos Z, Adamicza A, Asztalos T, Sly PD: Methacholine-induced bronchoconstriction in rats: effects of intravenous vs. aerosol delivery. *J Appl Physiol* (1985) 1997; 82: 1479-87
94. Lanteri CJ, Kano S, Sly PD: Validation of esophageal pressure occlusion test after paralysis. *Pediatr Pulmonol* 1994; 17: 56-62
95. Hantos Z, Daroczy B, Suki B, Nagy S, Fredberg JJ: Input impedance and peripheral inhomogeneity of dog lungs. *J Appl Physiol* (1985) 1992; 72: 168-78

96. Fredberg JJ, Stamenovic D: On the imperfect elasticity of lung tissue. *J Appl Physiol* (1985) 1989; 67: 2408-19
97. Crowley G, Kwon S, Caraher EJ, Haider SH, Lam R, Batra P, Melles D, Liu M, Nolan A: Quantitative lung morphology: semi-automated measurement of mean linear intercept. *BMC Pulm Med* 2019; 19: 206
98. Matute-Bello G, Winn RK, Jonas M, Chi EY, Martin TR, Liles WC: Fas (CD95) induces alveolar epithelial cell apoptosis in vivo: implications for acute pulmonary inflammation. *Am J Pathol* 2001; 158: 153-61
99. Chen CM, Juan SH, Pai MH, Chou HC: Hyperglycemia induces epithelial-mesenchymal transition in the lungs of experimental diabetes mellitus. *Acta Histochem* 2018; 120: 525-533
100. Schindelin J, Arganda-Carreras I, Frise E, Kaynig V, Longair M, Pietzsch T, Preibisch S, Rueden C, Saalfeld S, Schmid B, Tinevez JY, White DJ, Hartenstein V, Eliceiri K, Tomancak P, Cardona A: Fiji: an open-source platform for biological-image analysis. *Nat Methods* 2012; 9: 676-82
101. Janosi TZ, Adamicza A, Zosky GR, Asztalos T, Sly PD, Hantos Z: Plethysmographic estimation of thoracic gas volume in apneic mice. *J Appl Physiol* (1985) 2006; 101: 454-9
102. Villar J, Herrera-Abreu MT, Valladares F, Muros M, Perez-Mendez L, Flores C, Kacmarek RM: Experimental ventilator-induced lung injury: exacerbation by positive end-expiratory pressure. *Anesthesiology* 2009; 110: 1341-7
103. Yerevanian A, Soukas AA: Metformin: Mechanisms in Human Obesity and Weight Loss. *Curr Obes Rep* 2019; 8: 156-164
104. Lazzaroni E, Ben Nasr M, Loretelli C, Pastore I, Plebani L, Lunati ME, Vallone L, Bolla AM, Rossi A, Montefusco L, Ippolito E, Berra C, D'Addio F, Zuccotti GV, Fiorina P: Anti-diabetic drugs and weight loss in patients with type 2 diabetes. *Pharmacol Res* 2021; 171: 105782
105. Guo XX, Wang Y, Wang K, Ji BP, Zhou F: Stability of a type 2 diabetes rat model induced by high-fat diet feeding with low-dose streptozotocin injection. *J Zhejiang Univ Sci B* 2018; 19: 559-569
106. Wu KK, Huan Y: Streptozotocin-induced diabetic models in mice and rats. *Curr Protoc Pharmacol* 2008; Chapter 5: Unit 5 47
107. Choi HJ, Yeon MH, Jun HS: Schisandrae chinensis Fructus Extract Ameliorates Muscle Atrophy in Streptozotocin-Induced Diabetic Mice by Downregulation of the CREB-KLF15 and Autophagy-Lysosomal Pathways. *Cells* 2021; 10
108. Casey DT, Bou Jawde S, Herrmann J, Mori V, Mahoney JM, Suki B, Bates JHT: Percolation of collagen stress in a random network model of the alveolar wall. *Sci Rep* 2021; 11: 16654
109. Jones MG, Andriotis OG, Roberts JJ, Lunn K, Tear VJ, Cao L, Ask K, Smart DE, Bonfanti A, Johnson P, Alzetani A, Conforti F, Doherty R, Lai CY, Johnson B, Bourdakos KN, Fletcher SV, Marshall BG, Jogai S, Brereton CJ, Chee SJ, Ottensmeier CH, Sime P, Gauldie J, Kolb M, Mahajan S, Fabre A, Bhaskar A, Jarolimek W, Richeldi L, O'Reilly KM, Monk PD, Thurner PJ, Davies DE: Nanoscale dysregulation of collagen structure-function disrupts mechano-homeostasis and mediates pulmonary fibrosis. *Elife* 2018; 7
110. Pernicova I, Korbonits M: Metformin--mode of action and clinical implications for diabetes and cancer. *Nat Rev Endocrinol* 2014; 10: 143-56
111. Zmijewski JW, Lorne E, Zhao X, Tsuruta Y, Sha Y, Liu G, Siegal GP, Abraham E: Mitochondrial respiratory complex I regulates neutrophil activation and severity of lung injury. *Am J Respir Crit Care Med* 2008; 178: 168-79

112. Morales AI, Detaille D, Prieto M, Puente A, Briones E, Arevalo M, Lerverve X, Lopez-Novoa JM, El-Mir MY: Metformin prevents experimental gentamicin-induced nephropathy by a mitochondria-dependent pathway. *Kidney Int* 2010; 77: 861-9
113. Agard C, Rolli-Derkinderen M, Dumas-de-La-Roque E, Rio M, Sagan C, Savineau JP, Loirand G, Pacaud P: Protective role of the antidiabetic drug metformin against chronic experimental pulmonary hypertension. *Br J Pharmacol* 2009; 158: 1285-94
114. Sato N, Takasaka N, Yoshida M, Tsubouchi K, Minagawa S, Araya J, Saito N, Fujita Y, Kurita Y, Kobayashi K, Ito S, Hara H, Kadota T, Yanagisawa H, Hashimoto M, Utsumi H, Wakui H, Kojima J, Numata T, Kaneko Y, Odaka M, Morikawa T, Nakayama K, Kohrogi H, Kuwano K: Metformin attenuates lung fibrosis development via NOX4 suppression. *Respir Res* 2016; 17: 107
115. Zhang Q, Hu N: Effects of Metformin on the Gut Microbiota in Obesity and Type 2 Diabetes Mellitus. *Diabetes Metab Syndr Obes* 2020; 13: 5003-5014
116. Furman BL: Streptozotocin-Induced Diabetic Models in Mice and Rats. *Curr Protoc Pharmacol* 2015; 70: 5 47 1-5 47 20
117. Frank JA, Pittet JF, Wray C, Matthay MA: Protection from experimental ventilator-induced acute lung injury by IL-1 receptor blockade. *Thorax* 2008; 63: 147-53
118. Nieman GF, Gatto LA, Andrews P, Satalin J, Camporota L, Daxon B, Blair SJ, Al-Khalisy H, Madden M, Kollisch-Singule M, Aiash H, Habashi NM: Prevention and treatment of acute lung injury with time-controlled adaptive ventilation: physiologically informed modification of airway pressure release ventilation. *Ann Intensive Care* 2020; 10: 3
119. Andrade MC, Souza ABF, Horta JG, Paula Costa G, Talvani A, Cangussu SD, Menezes RCA, Bezerra FS: Applying Positive End-Expiratory Pressure During Mechanical Ventilation Causes Pulmonary Redox Imbalance and Inflammation in Rats. *Shock* 2018; 50: 572-578
120. Fisher AB, Dodia C, Chatterjee S: A Peptide Inhibitor of Peroxiredoxin 6 Phospholipase A(2) Activity Significantly Protects against Lung Injury in a Mouse Model of Ventilator Induced Lung Injury (VILI). *Antioxidants (Basel)* 2021; 10
121. Chen L, Xia HF, Shang Y, Yao SL: Molecular Mechanisms of Ventilator-Induced Lung Injury. *Chin Med J (Engl)* 2018; 131: 1225-1231
122. Giacco F, Brownlee M: Oxidative stress and diabetic complications. *Circ Res* 2010; 107: 1058-70
123. Foretz M, Hebrard S, Leclerc J, Zarrinpashneh E, Soty M, Mithieux G, Sakamoto K, Andreelli F, Viollet B: Metformin inhibits hepatic gluconeogenesis in mice independently of the LKB1/AMPK pathway via a decrease in hepatic energy state. *J Clin Invest* 2010; 120: 2355-69
124. Salminen A, Hyttinen JM, Kaarniranta K: AMP-activated protein kinase inhibits NF-kappaB signaling and inflammation: impact on healthspan and lifespan. *J Mol Med (Berl)* 2011; 89: 667-76
125. Hitchings AW, Lai D, Jones PW, Baker EH, Metformin in CTT: Metformin in severe exacerbations of chronic obstructive pulmonary disease: a randomised controlled trial. *Thorax* 2016; 71: 587-93
126. van den Berghe G, Wouters P, Weekers F, Verwaest C, Bruyninckx F, Schetz M, Vlasselaers D, Ferdinande P, Lauwers P, Bouillon R: Intensive insulin therapy in critically ill patients. *N Engl J Med* 2001; 345: 1359-67
127. Bar-Or D, Rael LT, Madayag RM, Banton KL, Tanner A, 2nd, Acuna DL, Lieser MJ, Marshall GT, Mains CW, Brody E: Stress Hyperglycemia in Critically Ill Patients: Insight Into Possible Molecular Pathways. *Front Med (Lausanne)* 2019; 6: 54
128. Wu CP, Huang KL, Peng CK, Lan CC: Acute Hyperglycemia Aggravates Lung Injury via Activation of the SGK1-NKCC1 Pathway. *Int J Mol Sci* 2020; 21

129. Chen Y, Zhang F, Wang D, Li L, Si H, Wang C, Liu J, Chen Y, Cheng J, Lu Y: Mesenchymal Stem Cells Attenuate Diabetic Lung Fibrosis via Adjusting Sirt3-Mediated Stress Responses in Rats. *Oxid Med Cell Longev* 2020; 2020: 8076105
130. Gheibi S, Kashfi K, Ghasemi A: A practical guide for induction of type-2 diabetes in rat: Incorporating a high-fat diet and streptozotocin. *Biomed Pharmacother* 2017; 95: 605-613
131. Garcia-Perez LE, Alvarez M, Dilla T, Gil-Guillen V, Orozco-Beltran D: Adherence to therapies in patients with type 2 diabetes. *Diabetes Ther* 2013; 4: 175-94
132. Wu CS, Chou HC, Huang LT, Lin YK, Chen CM: Bubble CPAP Support after Discontinuation of Mechanical Ventilation Protects Rat Lungs with Ventilator-Induced Lung Injury. *Respiration* 2016; 91: 171-9
133. Rogliani P, Lucà G, Lauro D: Chronic obstructive pulmonary disease and diabetes. *COPD Research and Practice* 2015; 1: 3